The Binding Energy of Nuclear Matter in the Chiral σ - ω Model

L. G. LIU, W. BENTZ, AND A. ARIMA

Department of Physics, Faculty of Science, University of Tokyo, Hongo, Bunkyo-ku, Tokyo 113, Japan

Received May 3, 1989

The binding energy of nuclear matter is calculated in the chiral σ - ω model in an approximation to the Hartree-Fock scheme. Relativistic exchange energies and correlation energies including the effects of vacuum polarization are calculated. It is found that if one includes only the nucleon loop term in the meson self-energies, no satisfactory description of nuclear matter can be given. It is argued that by including the meson loop terms in the meson self-energies one can account for the saturation properties of nuclear matter. © 1989 Academic Press, Inc.

1. Introduction

The description of nuclear matter and nuclei based on relativistic quantum field theory is a very challenging problem which attracted much attention especially during the last ten years. The starting point is a relativistic lagrangian describing the interaction of nucleons via the exchange of mesons [1, 2]. Although due to mainly technical difficulties it is at present still not possible to give a realistic description of strongly interacting systems within fully relativistic models, they endow us with a means to investigate the roles of mesonic degrees of freedom and the polarization of the negative energy Dirac sea, two points which cannot be studied unambiguously within a nonrelativistic framework.

The common ingredients of almost all relativistic models used so far to describe nuclear systems [2, 3] are the σ and the ω mesons coupling to the nucleons in order to account for the medium range attraction and the short-range repulsion in the nuclear force. Guided by the desire to incorporate the concept of chiral symmetry, in a recent paper [4] we thoroughly discussed the so-called chiral σ - ω model, which in addition includes the pion as well as nonlinear mesonic interaction terms. The lagrangian is given by the well-known linear σ model lagrangian to which the ω meson part including the usual vector coupling to the nucleon is added. From the theoretical side the model seems attractive, since it exhibits the constraints imposed by chiral symmetry on the energy density of the system in an explicit and illuminating way. Actual calculations of the nuclear matter binding energy within this model, however, are haunted by serious difficulties. It has been

known for a rather long time [6, 7] that in the simplest approximation, namely the quasiclassical approximation, it is not possible to describe saturating normal nuclear matter. Rather, one observes a chiral phase transition from the normal state (Goldstone mode of chiral symmetry) to the abnormal state (Wigner mode) at densities around the normal nuclear matter density. It is also well known [7] that in order to avoid this phase transition one has to include the contribution due to the negative energy Dirac sea to the energy density. The result is a saturating nuclear matter state and a continuous chiral phase transition at very high densities. In addition to this contribution of the Dirac sea, however, there are the "zero point oscillations" of the boson fields (π and σ) [1, 8]. It is not possible to assess these bosonic vacuum fluctuations as straightforwardly as the fermionic ones due to the presence of "tachyon poles" in the Hartree propagators of the bosons. In order to gain insight into the role of the zero-point oscillations of the σ field in the framework of the Hartree approximation, it is common [3] to add self-energy corrections to the σ propagator in a somewhat ad hoc way to prevent the tachyon pole. Strictly speaking, however, the presence of the tachyon poles renders the one loop (Hartree) calculation of the energy density impossible, and consequently people were led to investigate the two loop (Hartree-Fock) approximation [1, 4, 8, 9].

When we start from the Hartree-Fock expression for the energy density, the bosonic vacuum fluctuations discussed above are contained in the so-called "ring energies" (or RPA-type "correlation energies"). Their computation requires the self-consistent one loop (Hartree-Fock) meson propagators. The corresponding meson self-energies consist of the traditional particle-hole excitations, the nucleon-antinucleon excitations, and certain meson loop diagrams. The principal aim of the present paper is to study the role of these ring energies [9]. As a first step we consider only the ring energies due to the σ and ω mesons, leaving out the pionic contribution. The problems associated with the pion will be discussed, but not explored in detail. Relativistic ring energies have been considered theoretically in some works [1, 2, 10], but detailed investigations, especially in the framework of chiral models, have not yet been performed. An attempt has been made in Ref. [8] by using approximated forms of the meson self-energies.

In this work, the binding energy of nuclear matter including the contributions of the relativistic ring and exchange energies will be calculated. We start in Section 2 from the expression for the Hartree-Fock energy density as given in Ref. [4]. In order to make the calculation manageable, we omit the two line irreducible meson loop contributions to the energy density. Consequently, we start by considering the meson self-energies to be made up of particle-hole and nucleon-antinucleon loops. Consistently taking into account all relevant renormalization constants, we will demonstrate that the energy density, given in its final form by Eq. (2.49), is finite. The stability conditions for the RPA-type ring sum will be discussed. Usually the meson self-energy is decomposed [2] into a "density part" depending explicitly on the Fermi distribution function and a "Feynman part" describing vacuum polarization effects. In Section 3.1, we discuss the numerical results obtained by retaining

only the density parts in the meson self-energies. It will be shown that in this approximation nuclear matter is unstable at normal densities, and thus the saturation point lies at about half of the normal nuclear matter density (see Fig. 6). The reason for this will be discussed in detail. Then, in Section 3.2, we will re-include the Feynman parts of the meson self-energies in the calculation of the energy density. It will be shown that in this picture the nuclear matter binding energy does not saturate (see Fig. 13). The total binding energy and some individual contributions turn out to show a rather pathological behaviour. In Section 3.3, we will invoke the meson loop contributions to the meson self-energies and show that these cancel large parts of the nucleon loops. The physical reason for this cancellation will be discussed. We will estimate roughly the influence of these meson loops on the ring energies and find that saturation is recovered (see Fig. 20). A summary and conclusions are represented in Section 4.

The present work should be considered as a first step in the quantitative exploration of the effects of vacuum fluctuations on nuclear properties in chiral models based on the loop expansion technique. Many of the effects treated in this paper need further investigation. We emphasize that also the whole physical picture, as it emerges from a loop expansion, should be subject to discussion. In the course of the calculation we will be confronted with terms which become unphysically large when treated without phenomenological meson-nucleon vertex-form factors and, moreover, are very sensitive to assumed parameters. We therefore wish to leave open the possibility of alternative approaches which treat the effects of vacuum fluctuations more rigorously.

2. The Energy Density in the Chiral σ - ω Model

In this section we will derive the form of the energy density which will be used for the numerical calculations. The theoretical framework has been established in Ref. [4], and we will frequently refer to the results of that paper. For the sake of a self-contained presentation, however, we will first explain the essential ingredients of the model before turning to the energy density.

2.1. The Model

The lagrangian of the present model is obtained by adding the ω meson pieces to the familiar chiral σ model lagrangian [5]:

$$\mathcal{L} = \overline{\Psi} [i \nabla - g(\phi + i\pi \cdot \tau \gamma_5) - g_{\omega} \gamma_{\mu} V^{\mu}] \Psi + \frac{1}{2} [(\partial_{\mu} \phi)^2 + (\partial_{\mu} \pi)^2]$$

$$-\frac{1}{4} G_{\mu\nu} G^{\mu\nu} - \frac{\mu^2}{2} (\phi^2 + \pi^2) - \frac{\lambda^2}{4} (\phi^2 + \pi^2)^2 + \frac{m_{\omega}^2}{2} V_{\mu} V^{\mu} + c\phi. \tag{2.1}$$

This lagrangian consists of the fields Ψ , ϕ , π , and V^{μ} for the nucleon, the σ meson,

the pion, and the ω meson, respectively, and the coupling constants g, g_{ω} , and λ . We further introduced $G^{\mu\nu} = \partial^{\mu}V^{\nu} - \partial^{\nu}V^{\mu}$. The last term in (2.1) breaks the chiral symmetry explicitly, and c is the corresponding symmetry breaking parameter. The symmetry is spontaneously broken by assuming $\mu^2 < 0$. Since the σ and the ω meson fields have non-vanishing expectation values in the nuclear matter ground state, which we denote by \tilde{v} and \tilde{w}^{μ} , we translate the fields according to

$$\phi = \sigma + \tilde{v} \tag{2.2a}$$

$$V^{\mu} = \omega^{\mu} + \tilde{w}^{\mu}, \tag{2.2b}$$

defining the new quantum fields σ and ω^{μ} . The tilde in Eqs. (2.2) indicates the density dependence. The Green functions and accordingly also the energy density of the system calculated from the lagrangian (2.1) are generally divergent. In order to deal with these divergencies, we have to introduce renormalization constants for all fields, coupling constants and mass parameters in (2.1), which will be fixed by imposing renormalization conditions on the Green functions in free space (zero density). The renormalization procedure consistent with chiral symmetry has been discussed in Ref. [5] and applied to the case of nuclear matter in Ref. [4]. The final form of the lagrangian, after introducing Eqs. (2.2) and all renormalization constants into (2.1), is [4]

$$\mathcal{L} = \mathcal{L}_{MF} + \mathcal{L}_{L} + \mathcal{L}_{CT} \tag{2.3a}$$

with

$$\mathcal{L}_{\text{MF}} = -\frac{1}{4} \lambda^{2} Z_{\lambda} (\tilde{v}^{2} - v^{2})^{2} - \frac{m_{\pi}^{2} + \delta m_{\pi}^{2}}{2} (\tilde{v}^{2} - v^{2})$$

$$+ c(\tilde{v} - v) + \frac{m_{\omega}^{2} + \delta m_{\omega}^{2}}{2} \tilde{w}^{\mu} \tilde{w}_{\mu}$$

$$\mathcal{L}_{\text{L}} = \overline{\Psi} [i Z_{N} \nabla - \tilde{m}_{N} - \delta \tilde{m}_{N} - g Z_{g} (\sigma + i \pi \cdot \tau \gamma_{5}) - g_{\omega} Z_{g\omega} \gamma_{\mu} (\omega^{\mu} + \tilde{w}^{\mu})] \Psi$$

$$+ \frac{1}{2} [Z_{M} (\partial_{\mu} \sigma)^{2} - (\tilde{m}_{\sigma}^{2} + \delta \tilde{m}_{\sigma}^{2}) \sigma^{2}]$$

$$+ \frac{1}{2} [Z_{M} (\partial_{\mu} \pi)^{2} - (\tilde{m}_{\pi}^{2} + \delta \tilde{m}_{\pi}^{2}) \pi^{2}] - \frac{1}{4} Z_{\omega} G_{\mu\nu} G^{\mu\nu}$$

$$+ \frac{m_{\omega}^{2} + \delta m_{\omega}^{2}}{2} \omega_{\mu} \omega^{\mu} - \frac{1}{4} \lambda^{2} Z_{\lambda} (\sigma^{2} + \pi^{2})^{2} - \lambda^{2} Z_{\lambda} \tilde{v} \sigma (\sigma^{2} + \pi^{2})$$

$$\mathcal{L}_{\text{CT}} = \sigma (c - \tilde{v} (\tilde{m}_{\pi}^{2} + \delta \tilde{m}_{\pi}^{2})) + \omega_{\mu} \tilde{w}^{\mu} (m_{\omega}^{2} + \delta m_{\omega}^{2}).$$
(2.3d)

Here Z_N , Z_M and Z_{ω} are the wave function renormalization constants for the nucleon, the (σ, π) mesons, and the ω meson, and Z_g , Z_{λ} , and $Z_{g\omega}$ are the vertex renormalization constants for the σNN (and πNN) vertex, for the purely mesonic

interaction vertices and for the ωNN vertex, respectively. The lagrangian contains the density dependent mass parameters \tilde{m}_N , \tilde{m}_{σ}^2 , and \tilde{m}_{π}^2 together with their counterterms, as well as the mass renormalization counterterm δm_{ω}^2 for the ω meson. The lagrangian (2.3a) has been split into three parts, where \mathcal{L}_{MF} is a constant depending on the "mean fields" \tilde{v} and \tilde{w}^{μ} , \mathcal{L}_{L} is that part which will generate the loop terms in the energy density, and \mathcal{L}_{CT} is a counterterm which ensures that the fields σ and ω^{μ} have vanishing expectation values in the nuclear matter ground state, according to their definitions (2.2).

We now briefly discuss the definitions of all the parameters appearing in (2.3). Considering the masses m_N , m_π , and m_ω of the nucleon, the pion, and the ω meson in free space as fixed, the only free parameters are the σ meson mass m_σ and the ωNN coupling constant g_ω . The coupling constants g and λ are defined by the relations

$$m_N = gv \tag{2.4a}$$

$$m_{\sigma}^2 - m_{\pi}^2 = 2\lambda^2 v^2,$$
 (2.4b)

where v is the vacuum expectation value of ϕ , which is determined by symmetry requirements (see later). The density-dependent mass parameters are defined by

$$\tilde{m}_N = g\tilde{v} = m_N \frac{\tilde{v}}{v} \tag{2.5a}$$

$$\tilde{m}_{\sigma}^{2} = m_{\sigma}^{2} + 3\lambda^{2}(\tilde{v}^{2} - v^{2}) \tag{2.5b}$$

$$\tilde{m}_{\pi}^{2} = m_{\pi}^{2} + \lambda^{2} (\tilde{v}^{2} - v^{2}). \tag{2.5c}$$

The mass counterterms in free space δm_N , δm_{σ}^2 , δm_{π}^2 , and δm_{ω}^2 together with the wave function renormalization constants Z_N , Z_M , and Z_{ω} are determined in the usual way by imposing renormalization conditions on the single particle propagators. Throughout this work we will use the renormalization points $q^2 = m_N^2$ for the nucleon and $q^2 = 0$ for the mesons; i.e., we impose the following seven conditions on the renormalized self-energies in free space (characterized by a subscript f):

$$\Sigma_{Nf}(\mathbf{k} = \mathbf{m}_N) = \frac{\partial \Sigma_{Nf}}{\partial \mathbf{k}} (\mathbf{k} = \mathbf{m}_N) = 0$$
 (2.6a)

$$\Sigma_{\sigma f}(k^2 = 0) = \Sigma_{\pi f}(k^2 = 0) = \frac{\partial \Sigma_{\pi f}}{\partial k^2}(k^2 = 0) = 0$$
 (2.6b)

$$\sum_{Tf}(k^2=0) = \frac{\partial \Sigma_{Tf}}{\partial k^2}(k^2=0) = 0.$$
 (2.6c)

Here Σ_{Tf} is the transverse part of the ω meson self-energy in free space. The prescription (2.6c) together with baryon current conservation gives [11]

$$\delta m_{\omega}^2 = 0, \qquad Z_{g\omega} = Z_N. \tag{2.7}$$

The mass renormalization constants in free space, which are now fixed by Eqs. (2.6), in turn determine the vertex renormalization constants Z_g and Z_{λ} as well as the density-dependent mass counterterms

$$Z_g = 1 + \frac{\delta m_N}{m_N} \tag{2.8a}$$

$$Z_{\lambda} = 1 + \frac{\delta m_{\sigma}^{2} - \delta m_{\pi}^{2}}{m_{\sigma}^{2} - m_{\pi}^{2}},$$
 (2.8b)

$$\delta \tilde{m}_N = g(Z_g - 1)\tilde{v} = \delta m_N \frac{\tilde{v}}{v}$$
 (2.9a)

$$\delta \tilde{m}_{\alpha}^{2} = \delta m_{\alpha}^{2} + 3\lambda^{2}(Z_{\lambda} - 1)(\tilde{v}^{2} - v^{2})$$
 (2.9b)

$$\delta \tilde{m}_{\pi}^{2} = \delta m_{\pi}^{2} + \lambda^{2} (Z_{\lambda} - 1)(\tilde{v}^{2} - v^{2}).$$
 (2.9c)

The "mean fields" \tilde{v} and \tilde{w}^{μ} are determined as follows [4]: Baryon current conservation gives

$$\tilde{w}^{\mu} = \frac{g_{\omega}}{m_{\omega}^2} j_{B}^{\mu}, \tag{2.10}$$

where j_B^{μ} is the baryon current in the nuclear matter ground state. Since in the following we will work in the nuclear matter rest frame, we have $\tilde{\mathbf{w}} = \mathbf{j}_B = 0$. The partial conservation of the axial vector current (PCAC) gives the implicit relation (the Goldstone theorem) to determine \tilde{v} ,

$$-\tilde{v}\Delta_{\pi}^{-1}(0) = \tilde{v}(\tilde{m}_{\pi}^{2} + \Sigma_{\pi}(0)) = c, \tag{2.11}$$

where $\Delta_{\pi}(q)$ ($\Sigma_{\pi}(q)$) is the renormalized pion propagator (self-energy) in the nuclear medium. The symmetry-breaking parameter is generally related to pionic properties by $c = F_{\pi} M_{\pi}^2$, where F_{π} is the pion decay constant and M_{π} is the pole position of the pion propagator in free space. On the other hand, due to the renormalization prescription (2.6b), Eq. (2.11) in free space becomes $c = v m_{\pi}^2$, and hence v is determined to be $v = F_{\pi} M_{\pi}^2 / m_{\pi}^2$. An explicit one loop calculation of the pion self-energy shows that [5] $M_{\pi} \approx m_{\pi}$, and therefore $v \approx F_{\pi}$. From Eq. (2.4a), the coupling constant g then takes the value $g \approx 10$. We will use the value g = 10 throughout this paper.

2.2. Form of the Energy Density

We start from the self-consistent two loop (Hartree-Fock) expression for the energy density, which was derived in Ref. [4] from the lagrangian (2.3):

$$E = U + \delta U + E_r + E_t. \tag{2.12}$$

Here U is the familiar two-humped "potential" including the contribution from the ω mean field,

$$U = \frac{m_{\sigma}^2 - m_{\pi}^2}{8v^2} (\tilde{v}^2 - v^2)^2 + \frac{m_{\pi}^2}{2} (\tilde{v}^2 - v^2) - c(\tilde{v} - v) - \frac{m_{\omega}^2}{2} \tilde{w}_0^2, \tag{2.13}$$

and δU is the counterterm

$$\delta U = -VEV + \frac{\delta m_{\sigma}^2 - \delta m_{\pi}^2}{8v^2} (\tilde{v}^2 - v^2)^2 + \frac{\delta m_{\pi}^2}{2} (\tilde{v}^2 - v^2).$$
 (2.14)

It includes the subtraction of the vacuum expectation value (VEV) in order that E of Eq. (2.12) vanish for zero density. The "ring energy" E_r is given by

$$E_r = E_{N}'' + E_{\sigma \omega}'' + E_{\tau}'' \tag{2.15a}$$

with

$$E_{N}' = -i \int \frac{d^{4}k}{(2\pi)^{4}} \operatorname{Tr}(\ln(S_{f}^{-1}S) - \overline{S}_{0}^{-1}S)$$
 (2.15b)

$$E_{\sigma\omega}' = \frac{i}{2} \int \frac{d^4k}{(2\pi)^4} \operatorname{Tr}(\ln(\Delta_f^{-1}\Delta) - \overline{\Delta}_0^{-1}\Delta)$$
 (2.15c)

$$E_{\pi}' = \frac{3i}{2} \int \frac{d^4k}{(2\pi)^4} \left(\ln(\Delta_{\pi f}^{-1} \Delta_{\pi}) - \bar{\Delta}_{\pi 0}^{-1} \Delta_{\pi} \right). \tag{2.15d}$$

Here S and Δ_{π} are the full renormalized propagators for the nucleon and the pion, and Δ is the combined propagator for σ and ω defined in Ref. [4]. The propagators characterized by f are the full renormalized propagators in free space, and

$$\overline{S}_0(k) = \frac{1}{Z_N \widetilde{k} - \widetilde{m}_N - \delta \widetilde{m}_N + i\delta_k}$$
 (2.16a)

$$\bar{\Delta}_{0}^{ab} = \begin{cases} \bar{\Delta}_{\sigma 0} = \frac{1}{Z_{M}k^{2} - \tilde{m}_{\sigma}^{2} - \delta\tilde{m}_{\sigma}^{2}} & \text{for } a = b = -1\\ g^{\mu\nu}\bar{\Delta}_{\omega 0} = g^{\mu\nu} \frac{-1}{Z_{\omega}k^{2} - m_{\omega}^{2}} & \text{otherwise} \end{cases}$$
(2.16b)

$$\bar{\Delta}_{\pi 0} = \frac{1}{Z_M k^2 - \tilde{m}_{\pi}^2 - \delta \tilde{m}_{\pi}^2}.$$
 (2.16c)

In (2.16a) we used

$$\tilde{k}^{\mu} = k^{\mu} - g_{\omega} \tilde{w}^{\mu}, \qquad \delta_k = \delta(1 - 2n(k) \theta(k_0))$$

with n(k) the Fermi distribution and $\delta > 0$ an infinitesimal quantity. The roman

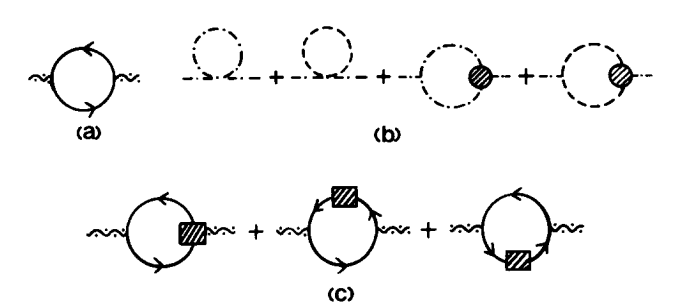


Fig. 1. The one-loop (Hartree-Fock) combined self-energy for σ and ω mesons, expanded in terms of the nucleon Hartree propagator (full line). The meson lines refer to the RPA meson propagators. The wavy line with dots denotes the σ or ω meson, and the dashed and dashed-dotted lines represent the π and σ mesons, respectively. The circles stand for vertices, and the squares for vertex and self-energy corrections.

indices (a, b) of the combined propagator Δ take the values -1 to 3, where the index -1 characterizes the σ meson degree of freedom, and the Greek indices run from 0 to 3. Finally, the loop contribution in (2.12) is given by

$$E_{l} = \frac{i}{2} \int \frac{d^{4}k}{(2\pi)^{4}} \left(\operatorname{Tr}(\Delta \bar{\Sigma}) + 3\Delta_{\pi} \bar{\Sigma}_{\pi} \right) + E_{l, \text{mes}}. \tag{2.17}$$

The first term in (2.17) is the familiar Fock term, while $E_{l,\text{mes}}$ is the contribution of the purely mesonic loops. The unrenormalized self-energies $\bar{\Sigma}$ and $\bar{\Sigma}_{\pi}$ in (2.17) are shown graphically by the diagrams in Figs. 1a and 2a, respectively, if the full lines are considered as the self-consistent Hartree-Fock propagators. Equation (2.17) is the two-loop term in the expansion of the energy density with respect to the number of loops.

The variation of the energy density (2.12) with respect to the propagators S, Δ , and Δ_{π} gives the Dyson equations, which are in general coupled integral equations. The presence of divergencies makes an exact solution of these integral equations very difficult. The main purpose of this paper is to investigate if one can achieve

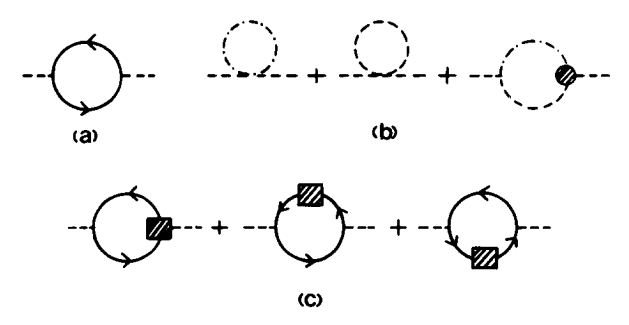


Fig. 2. Same as Fig. 1 for the pion self-energy.

a satisfactory description of the nuclear matter binding energy by making the following two simplifications: First, to neglect the meson loops in (2.17), i.e.,

$$E_{l,\text{mes}} = 0, \tag{2.18}$$

and, second, to construct the meson self energies in (2.17) or Figs. 1a, 2a by using the lowest order (Hartree) nucleon propagator S_0 , which is given by (2.16a) with $Z_N = \delta \tilde{m}_N = 0$. In order to be consistent with this latter approximation, we also have to replace $S \to S_0$ in the counterterm contribution of (2.15b), i.e.,

$$\overline{S}_0^{-1}S = (S_0^{-1} + (Z_N - 1)\tilde{k} - \delta \tilde{m}_N) S \to S_0^{-1}S + ((Z_N - 1)\tilde{k} - \delta \tilde{m}_N)S_0.$$
 (2.19)

With these two approximations we obtain the Dyson equations by varying (2.12) with respect to S, Δ , and Δ_{π} ,

$$S = S_0 \tag{2.20a}$$

$$\Delta = \overline{\Delta}_0 + \overline{\Delta}_0 \overline{\Sigma} \Delta = \Delta_f + \Delta_f \Pi \Delta \tag{2.20b}$$

$$\Delta_{\pi} = \overline{\Delta}_{\pi 0} + \overline{\Delta}_{\pi 0} \overline{\Sigma}_{\pi} \Delta_{\pi} = \Delta_{\pi f} \Pi_{\pi} \Delta_{\pi}$$
 (2.20c)

with

$$\Pi^{ab} = \Sigma^{ab} - \Sigma_f^{ab} + \delta^{a-1}\delta^{b-1}\delta_{\sigma}$$
 (2.21a)

$$\Pi_{\pi} = \Sigma_{\pi} - \Sigma_{\pi f} + \delta_{\pi} \tag{2.21b}$$

$$\delta_{\sigma} = \tilde{m}_{\sigma}^{2} - m_{\sigma}^{2}; \qquad \delta_{\pi} = \tilde{m}_{\pi}^{2} - m_{\pi}^{2}.$$
 (2.21c)

The meson self-energies Σ here are the renormalized nucleon-loop contributions (specified below) constructed from the Hartree propagator S_0 . Note that Δ_f and $\Delta_{\pi f}$ in Eqs. (2.20) include the self-energies in free space, and therefore the latter ones are subtracted in Eqs. (2.21).

Due to the Dyson equations (2.20b), (2.20c) the last terms in (2.15c), (2.15d) cancel against the loop term (2.17), and we are left with

$$E = U + \delta U + E_{\rm L} \tag{2.22a}$$

with

$$E_{L} = -i \int \frac{d^{4}k}{(2\pi)^{4}} \operatorname{Tr} \ln(S_{0f}^{-1}S_{0}) + \frac{i}{2} \int \frac{d^{4}k}{(2\pi)^{4}} \operatorname{Tr} \ln(\Delta_{f}^{-1}\Delta) + \frac{3i}{2} \int \frac{d^{4}k}{(2\pi)^{4}} \ln(\Delta_{\pi f}^{-1}\Delta_{\pi}) - i \int \frac{d^{4}k}{(2\pi)^{4}} \operatorname{Tr}(S_{0}(\delta \tilde{m}_{N} - \tilde{k}(Z_{N} - 1))). \quad (2.22b)$$

Let us now discuss the counterterm contribution δU . Since E is required in the two loop approximation, one could in principle consider the σ and π self-energies in free space in the same approximation to calculate the mass counterterms δm_{π}^2 and δm_{σ}^2

required in Eq. (2.14). Due to our renormalization conditions (2.6) one can, however, calculate these mass counterterms more conveniently directly from the expression (2.22) for the energy density. For this purpose we use the general relations, which hold for any fixed density.

$$\frac{\partial E}{\partial \tilde{v}} = -\tilde{v} \, \Delta_{\pi}^{-1}(0) - c = \tilde{v}(\tilde{m}_{\pi}^2 + \delta \tilde{m}_{\pi}^2 + \bar{\Sigma}_{\pi}(0)) - c \tag{2.23a}$$

$$\frac{\partial^2 E}{\partial \tilde{v}^2} = -\Delta_{\sigma}^{-1}(0) = \tilde{m}_{\sigma}^2 + \delta \tilde{m}_{\sigma}^2 + \bar{\Sigma}_{\sigma}(0), \tag{2.23b}$$

which were exploited extensively in Ref. [4]. Equation (2.23a) states that, for exact chiral symmetry (c=0), the minimization of E with respect to \tilde{v} at fixed density leads either to a pole in the pion propagator at q=0 (Goldstone mode) or to a vanishing value for \tilde{v} and \tilde{m}_N (Wigner mode). The minimization condition obtained from (2.23a) thus agrees with the Goldstone theorem (2.11). Due to Eq. (2.23b), the condition $-\Delta_{\sigma}^{-1}(0)>0$ decides which of the two modes is actually realized. Although we use the same notations, note that the propagators and self-energies in (2.23) also contain the two loop contributions (since we calculate E in the two loop approximation), in contrast to the quantities in (2.20) and (2.21). In Appendix A we demonstrate the relations (2.23), i.e., we derive the two loop expressions for the σ and π self-energies which are consistent with the expression (2.22) for the energy density.

Using (2.23) in the free space limit (density $\rho \to 0$, $\tilde{v} \to v$) we obtain, using (2.22a) (see also Eqs. (A.1) and (A.12))

$$\left. \frac{\partial E_L}{\partial \tilde{v}} \right|_{\rho = 0, \tilde{v} = v} = v \bar{\Sigma}_{\pi f}(0) = -v \delta m_{\pi}^2$$
 (2.24a)

$$\left. \frac{\partial^2 E_L}{\partial \tilde{v}^2} \right|_{\rho = 0, \tilde{v} = v} = \bar{\Sigma}_{\sigma f}(0) = -\delta m_{\sigma}^2, \tag{2.24b}$$

where in the second steps we used the renormalization conditions (2.6b). Equation (2.24) determines the mass counterterms δm_{π}^2 and δm_{σ}^2 in terms of E_L . Due to chiral symmetry, E_L depends only on \tilde{v}^2 rather than on \tilde{v} . Using this fact we obtain, on putting (2.24) into (2.14),

$$\delta U = -E_L|_{\rho = 0, \tilde{v} = v} - (\tilde{v}^2 - v^2) \frac{\partial E_L}{\partial \tilde{v}^2}|_{\rho = 0, \tilde{v} = v} - \frac{1}{2} (\tilde{v}^2 - v^2)^2 \frac{\partial^2 E_L}{\partial (\tilde{v}^2)^2}|_{\rho = 0, \tilde{v} = v}. \tag{2.25}$$

This expression shows that the counterterm δU effectively subtracts the first three terms in the expansion of E_L for $\rho = 0$ around $\tilde{v}^2 = v^2$. Therefore, the total energy density E for $\rho = 0$ behaves like $(\tilde{v}^2 - v^2)^3$ as $\tilde{v} \to v$.

The aim of the rest of this section is to bring the energy density (2.22) into a form more clearly showing its finiteness and its physical content. Our final result will be

given by Eq. (2.49). Since in the actual calculation we will not include the pionic contribution in (2.22b), we shall omit it in the following formulae. (Problems associated with the inclusion of the pionic contribution will be discussed in Section 4.) It is convenient to split the Hartree propagator S_0 into two parts [2]

$$S_0 = S_{0F} + S_{0D} \tag{2.26a}$$

with the "Feynman part"

$$S_{0F} = \frac{1}{\tilde{k} - \tilde{m}_N + i\delta}$$
 (2.26b)

and the "density part"

$$S_{0D} = (\tilde{k} + \tilde{m}_N) \pi i \frac{n(k)}{\tilde{E}_k} \delta(\tilde{k}_0 - \tilde{E}_k)$$
 (2.26c)

with $\tilde{E}_k = \sqrt{\mathbf{k}^2 + \tilde{m}_N^2}$. Then the nucleonic part in (2.22b) can be treated as in Ref. [4] with the result

$$-i \int \frac{d^4k}{(2\pi)^4} \operatorname{Tr} \ln(S_{0f}^{-1}S_0) = 4 \int \frac{d^3k}{(2\pi)^3} \tilde{E}_k n(k) + g_{\omega} \tilde{w}^0 \rho$$
$$+4i \int \frac{d^4k}{(2\pi)^4} \ln\left(1 - \frac{\delta_N}{k^2 - m_N^2 + i\delta}\right) \qquad (2.27a)$$

with

$$\delta_N = \tilde{m}_N^2 - m_N^2. {(2.27b)}$$

For the combined σ , ω contribution in (2.22b) we can write, using the Dyson equation (2.20b),

$$\frac{i}{2} \int \frac{d^4k}{(2\pi)^4} \operatorname{Tr} \ln(\Delta_f^{-1} \Delta) = -\frac{i}{2} \int \frac{d^4k}{(2\pi)^4} (\ln \varepsilon_{L} + 2 \ln \varepsilon_{T}), \tag{2.28a}$$

where we defined the longitudinal and transverse polarizabilities by [2]

$$\det(1 - \Pi \Delta_f) = \varepsilon_{\rm L} \varepsilon_{\rm T}^2. \tag{2.28b}$$

In order to derive their explicit expressions, we need the renormalized polarization insertions in (2.21a). They are given by (see Fig. 1a)

$$\Sigma^{-1-1}(k) = \Sigma_{\sigma}(k) = -ig^2 \int \frac{d^4q}{(2\pi)^4} \operatorname{Tr}(S_0(k+q) S_0(q)) + \delta \tilde{m}_{\sigma}^2 - k^2 (Z_M - 1)$$

$$= \Sigma_{\sigma D}(k) + \Sigma_{\sigma F}(k)$$
(2.29a)

$$\Sigma^{\mu\nu}(k) = \Sigma_{\omega}^{\mu\nu}(k) = -ig_{\omega}^{2} \int \frac{d^{4}q}{(2\pi)^{4}} \operatorname{Tr}(\gamma^{\mu}S_{0}(k+q)\gamma^{\nu}S_{0}(q))$$

$$-\left(g^{\mu\nu} - \frac{k^{\mu}k^{\nu}}{k^{2}}\right) (Z_{\omega} - 1)$$

$$= \Sigma_{\omega}D^{\mu\nu}(k) + \Sigma_{\omega}E^{\mu\nu}(k) \qquad (2.29b)$$

$$\Sigma^{\mu-1}(k) = \Sigma^{-1\mu}(k) = -igg_{\omega} \int \frac{d^4q}{(2\pi)^4} \operatorname{Tr}(\gamma^{\mu} S_0(k+q) S_0(q)). \tag{2.29c}$$

The "density parts" of these polarizations, characterized by a subscript D, involve at least one factor $S_{\rm 0D}$ in the integrals of (2.29), while the "Feynman parts" involve the combination $S_{\rm 0F}S_{\rm 0F}$ in the integrals and include also the counterterms. The combination $S_{\rm 0F}S_{\rm 0F}$ does not contribute in (2.29c). The polarizations satisfy the relations

$$k_{\mu} \Sigma^{\mu a}(k) = 0. \tag{2.30}$$

For future reference we note that the Feynman part of (2.29b) has the structure

$$\Sigma_{\omega F}^{\mu \nu} = \left(-g^{\mu \nu} + \frac{k^{\mu} k^{\nu}}{k^2}\right) \Sigma_{TF}, \qquad (2.31)$$

defining the transverse self-energy Σ_{TF} . (In free space it coincides with Σ_{Tf} of Eq. (2.6c).) Analogous to Eqs. (2.29) the polarizations Π of (2.21a) will be split as

$$\Pi^{-1-1} = \Pi_{\sigma} = \Pi_{\sigma D} + \Pi_{\sigma F} + \delta_{\sigma}$$
(2.32a)

with

$$\Pi_{\sigma D} = \Sigma_{\sigma D}
\Pi_{\sigma F} = \Sigma_{\sigma F} - \Sigma_{\sigma I};$$
(2.32b)

$$\Pi^{\mu\nu} = \Pi_{\alpha}^{\ \mu\nu} = \Pi_{\alpha}^{\ \mu\nu} + \Pi_{\alpha}^{\ \mu\nu}$$
 (2.32c)

with

$$\Pi_{\omega D}^{\mu \nu} = \Sigma_{\omega D}^{\mu \nu}
\Pi_{\omega F}^{\mu \nu} = \Sigma_{\omega F}^{\mu \nu} - \Sigma_{\omega f}^{\mu \nu};$$
(2.32d)

$$\Pi^{\mu-1} = \Sigma^{\mu-1}. (2.32e)$$

For the calculation of the determinant in (2.28b) it is convenient to choose **k** to lie on the x axis. Then the seven different non-vanishing components of Π^{ab} are Π^{-1-1} , Π^{00} , Π^{11} , $\Pi^{22} = \Pi^{33}$, $\Pi^{-10} = \Pi^{0-1}$, $\Pi^{-11} = \Pi^{1-1}$, and $\Pi^{01} = \Pi^{10}$. Equation (2.30) gives three relations (for a = -1, 0, 1), and we are left with four inde-

pendent components, which we will choose to be Π^{-1-1} , Π^{00} , Π^{33} , and Π^{0-1} . Noting that the free-space propagator Δ_f has the same tensor structure as the unrenormalized propagator (2.16b), one can calculate the determinant explicitly with the result

$$\varepsilon_{L} = (1 - \Delta_{\sigma f} \Pi_{\sigma})(1 - \Delta_{\omega f} \Pi_{L}) - \Delta_{\sigma f} \Delta_{\omega f} \Pi_{M}^{2}$$
 (2.33a)

$$\varepsilon_{\rm T} = 1 + \Delta_{\rm \omega f} \Pi_{\rm T} \tag{2.33b}$$

with the free space propagators

$$\Delta_{f}^{-1-1} = \Delta_{\sigma f} = \frac{1}{k^2 - m_{\sigma}^2 - \Sigma_{\sigma f}(k)}$$
 (2.34a)

$$\Delta_{\rm f}^{\mu\nu} = g^{\mu\nu} \Delta_{\omega f} = g^{\mu\nu} \frac{-1}{k^2 - m_{\omega}^2 - \Sigma_{\rm Tf}(k)}.$$
 (2.34b)

 Π_{σ} has been introduced in (2.32a), and the other quantities in (2.33) are defined by

$$\Pi_{L} = \Pi_{\omega}^{00} - \Pi_{\omega}^{11} = -\frac{k^{2}}{|\mathbf{k}|^{2}} \Pi_{\omega}^{00}$$
 (2.35a)

$$\Pi_{\mathsf{M}}^{2} = \Pi_{0-1}^{2} - \Pi_{1-1}^{2} = -\frac{k^{2}}{|\mathbf{k}|^{2}} \Pi_{0-1}^{2}$$
 (2.35b)

$$\Pi_{\mathsf{T}} = \Pi_{\omega}^{33}.\tag{2.35c}$$

Here L and T stand for the longitudinal and transverse part of the ω meson polarizations, and M denotes the mixed polarization with one external σ and one external ω meson leg. Equation (2.30) was used in deriving the second equalities in (2.35a, 2.35b). By using (2.32d) we will also split the longitudinal and transverse polarizations introduced above into their Feynman and density parts:

$$\Pi_{L} = \Pi_{LF} + \Pi_{LD} \tag{2.36a}$$

$$\Pi_{\rm T} = \Pi_{\rm TF} + \Pi_{\rm TD}.$$
 (2.36b)

Note that due to the structure of (2.31) we have, for the Feynman parts,

$$\Pi_{\rm TF} = -\Pi_{\rm LF} = \Sigma_{\rm TF} - \Sigma_{\rm Tf}. \tag{2.36c}$$

Inserting Eqs. (2.33) into (2.28a) one obtains the expression for the combined σ , ω contribution to the energy density.

Next we turn to the last term in (2.22b). We first note that the factor \tilde{k} in the integrand can be replaced by \tilde{m}_N : If the density part of the Hartree propagator, Eq. (2.26c), is inserted into this term, the δ function leaves only the on-shell value of the integrand, which means effectively $\tilde{k} \to \tilde{m}_N$ in the last term of (2.22b). When the Feynman part (2.26b) is inserted we have, after a shift of the integration

variable, $\text{Tr}(S_{\text{of}} \tilde{k}) \propto k^2/(k^2 - \tilde{m}_{\text{N}}^2) = 1 + \tilde{m}_{\text{N}}^2/(k^2 - \tilde{m}_{\text{N}}^2)$, and the "1" in this last expression is cancelled by the subtraction of the VEV. We further use

$$\delta \tilde{m}_{\mathrm{N}} - \tilde{m}_{\mathrm{N}}(Z_{\mathrm{N}} - 1) = \frac{\tilde{m}_{\mathrm{N}}}{m_{\mathrm{N}}} \left(\delta m_{\mathrm{N}} - m_{\mathrm{N}}(Z_{\mathrm{N}} - 1) \right) = -\frac{\tilde{m}_{\mathrm{N}}}{m_{\mathrm{N}}} \left. \overline{\Sigma}_{\mathrm{Nf}} \right|_{\phi = m_{\mathrm{N}}}. \tag{2.37}$$

Here the first equality follows from Eq. (2.9a) and the second one from the renormalization condition (2.6a). Note that $\bar{\Sigma}_{Nf}$ denotes the unrenormalized nucleon self-energy in free space. Therefore, the last term in (2.22b) becomes

$$-i \int \frac{d^{4}k}{(2\pi)^{4}} \operatorname{Tr}(S_{0}(\delta \tilde{m}_{N} - \tilde{k}(Z_{N} - 1)))$$

$$= i \frac{\tilde{m}_{N}}{m_{N}} \bar{\Sigma}_{Nf} \bigg|_{\dot{p} = m_{N}} \left(\int \frac{d^{4}k}{(2\pi)^{4}} \operatorname{Tr} S_{0D} + i \frac{\tilde{m}_{N}^{3}}{2\pi^{2}} \left(a - \ln \frac{\tilde{m}_{N}^{2}}{m_{N}^{2}} \right) \right). \tag{2.38}$$

Here we have performed the integral over S_{0F} , and the divergent constant a is given by

$$a = \Gamma(2 - \frac{n}{2}) + 1 - \ln m_N^2$$

where Γ is the gamma function and n the number of dimensions.

So far we discussed the forms of the various terms in Eq. (2.22b). The results are given by Eqs. (2.27a), (2.28a), and (2.38). From these formulae one can directly calculate the counterterm δU of Eq. (2.25). For this we note that for zero density $(\rho=0)$, but $\tilde{v}\neq v$ the polarizabilities (2.33) involve only the Feynman parts of the polarizations and the mass shift δ_{σ} of Eq. (2.21c). A simple calculation gives

$$\delta U = 4i \int \frac{d^4k}{(2\pi)^4} \left(\frac{\delta_{\rm N}}{k^2 - m_{\rm N}^2} + \frac{1}{2} \left(\frac{\delta_{\rm N}}{k^2 - m_{\rm N}^2} \right)^2 \right)$$
 (2.39a)

$$-\frac{i}{2}\int \frac{d^4k}{(2\pi)^4} \left\{ \Delta_{\sigma f} \left(\delta_{\sigma} + \delta_{N} \Sigma_{\sigma f}' + \frac{1}{2} \delta_{N}^{2} \Sigma_{\sigma F}'' \right) + \frac{1}{2} \left[\Delta_{\sigma f} (\delta_{\sigma} + \delta_{N} \Sigma_{\sigma F}') \right]^{2} \right\}$$
(2.39b)

$$-\frac{3i}{2}\int \frac{d^4k}{(2\pi)^4} \left\{ \Delta_{\omega f} \left(\delta_N \Sigma_{TF} + \frac{1}{2} \delta_N^2 \Sigma_{TF}'' \right) + \frac{1}{2} \left[\Delta_{\omega f} \delta_N \Sigma_{TF}' \right]^2 \right\}$$
 (2.39c)

$$-\frac{1}{2\pi^{2}} \frac{\bar{\Sigma}_{Nf}}{m_{N}} \bigg|_{\delta = m_{N}} \left(-\tilde{m}_{N}^{4} a + m_{N}^{2} \delta_{N} + \frac{3}{2} \delta_{N}^{2} \right). \tag{2.39d}$$

Here, as in the following, we use the notation

$$A' = \frac{\partial A}{\partial \tilde{m}_{N}^{2}} \Big|_{\tilde{m}_{N}^{2} = m_{N}^{2}}, \qquad A'' = \frac{\partial^{2} A}{\partial (\tilde{m}_{N}^{2})^{2}} \Big|_{\tilde{m}_{N}^{2} = m_{N}^{2}}.$$
 (2.40)

The term (2.39a) comes from the nucleonic contribution in (2.22b); (2.39b) and

(2.39c) have been derived from the (σ, ω) contribution in (2.22b); and (2.39d) has been derived from the last term in (2.22b). The mass shift δ_N is given by (2.27b).

We have now derived the explicit forms of all the terms in the energy density (2.22), and it remains to add them together in such a way that the finiteness of the whole expression becomes evident. For this, let us first separate the divergent parts from the expressions (2.27a) and (2.28a). For (2.27a) we write

$$-i \int \frac{d^4k}{(2\pi)^4} \operatorname{Tr} \ln(S_{0f}^{-1}S_0) = 4 \int \frac{d^3k}{(2\pi)^3} \tilde{E}_k n(k) + g_{\omega} \tilde{w}^0 \rho + E_N^C + \delta E_N \quad (2.41a)$$

with

$$E_{N}^{C} = 4i \int \frac{d^{4}k}{(2\pi)^{4}} \left\{ \ln \left(1 - \frac{\delta_{N}}{k^{2} - m_{N}^{2}} \right) + \frac{\delta_{N}}{k^{2} - m_{N}^{2}} + \frac{1}{2} \left(\frac{\delta_{N}}{k^{2} - m_{N}^{2}} \right)^{2} \right\}$$
 (2.41b)

$$\delta E_{\rm N} = -4i \int \frac{d^4k}{(2\pi)^4} \left\{ \frac{\delta_{\rm N}}{k^2 - m_{\rm N}^2} + \frac{1}{2} \left(\frac{\delta_{\rm N}}{k^2 - m_{\rm N}^2} \right)^2 \right\}. \tag{2.41c}$$

The term E_N^C is finite, and the divergent term δE_N is cancelled by (2.39a). Next consider (2.28a). The density parts of the polarizations Π in (2.33) go as $1/k^2$ for $k \to \infty$ [2], while Feynman parts, as we will see later, behave as $\ln k^2$ in this limit. Consequently, we write

$$\frac{i}{2} \int \frac{d^4k}{(2\pi)^4} \operatorname{Tr} \ln(\Delta_f^{-1} \Delta) = E_L^C + E_T^C + \delta E_{2D} + \delta E_{2F} + \delta E_4$$
 (2.42a)

with

$$E_{\rm L}^{C} = -\frac{i}{2} \int \frac{d^4k}{(2\pi)^4} \left\{ \ln \varepsilon_{\rm L} + \Delta_{\sigma \rm f} \Pi_{\sigma} + \Delta_{\omega \rm f} \Pi_{\rm L} + \frac{1}{2} \left(\Delta_{\sigma \rm f} (\delta_{\sigma} + \Pi_{\sigma \rm F}) \right)^2 + \frac{1}{2} \left(\Delta_{\omega \rm f} \Pi_{\rm LF} \right)^2 \right\}$$
(2.42b)

$$E_{\rm T}{}^{C} = -i \int \frac{d^4k}{(2\pi)^4} \left\{ \ln \varepsilon_{\rm T} - \Delta_{\omega f} \Pi_{\rm T} + \frac{1}{2} (\Delta_{\omega f} \Pi_{\rm TF})^2 \right\}$$
 (2.42c)

$$\delta E_{2D} = \frac{i}{2} \int \frac{d^4k}{(2\pi)^4} (\Delta_{\sigma f} \Pi_{\sigma D} + \Delta_{\omega f} \Pi_{LD} - 2\Delta_{\omega f} \Pi_{TD})$$

$$= \frac{i}{2} \int \frac{d^4k}{(2\pi)^4} \left(\Delta_{\sigma f} \Sigma_{\sigma D} + \left(\Delta_{\omega f} \Sigma_{\omega D} \right)^{\mu}_{\mu} \right) \tag{2.42d}$$

$$\delta E_{2F} = \frac{i}{2} \int \frac{d^4k}{(2\pi)^4} \left(\Delta_{\sigma f} \Pi_{\sigma F} + \Delta_{\omega f} \Pi_{LF} - 2\Delta_{\omega f} \Pi_{TF} \right)$$
 (2.42e)

$$\delta E_4 = \frac{i}{4} \int \frac{d^4k}{(2\pi)^4} \left\{ (\Delta_{\sigma f} (\delta_{\sigma} + \Pi_{\sigma F}))^2 + (\Delta_{\omega f} \Pi_{LF})^2 + 2(\Delta_{\omega f} \Pi_{TF})^2 \right\}. \tag{2.42f}$$

The terms E_L^C and E_T^C are finite, while the terms δE_2 of second order and δE_4 of fourth order in the coupling constants are divergent. We have to combine them with the contributions (2.38) and (2.39) in order to get a finite result. Consider first the term (2.42d). As explained before, the density parts of the self-energies involve at least one factor S_{0D} in the integrals of (2.29). The combination $S_{0D}S_{0D}$ will give rise to a finite result when inserted into (2.42d). The resulting contribution is the familiar exchange term, which we will call $E_{(1)}^{ex}$ (see Eq. (2.45b) below). The remaining terms involve the combination $S_{0F}S_{0D}$ and, when inserted into (2.42d), give

$$-i\int \frac{d^4k}{(2\pi)^4} \operatorname{Tr}(\bar{\Sigma}_{NF} S_{0D}) = -i\bar{\Sigma}_{NF}|_{\tilde{k} = \tilde{m}_N} \int \frac{d^4k}{(2\pi)^4} \operatorname{Tr} S_{0D}.$$
 (2.43)

Here $\bar{\Sigma}_{NF}$ is the unrenormalized "Feynman part" of the nucleon self-energy (see Fig. 3):

$$\bar{\Sigma}_{\rm NF}(k) = ig^2 \int \frac{d^4k}{(2\pi)^4} S_{\rm 0F}(q) \, \Delta_{\rm of}(k-q) + ig_{\omega}^2 \int \frac{d^4k}{(2\pi)^4} \gamma_{\mu} S_{\rm 0F}(q) \, \gamma^{\mu} \Delta_{\rm of}(k-q). \tag{2.44}$$

It is a manifestly Lorentz invariant function, and when we expand it around $\tilde{k} = \tilde{m}_{\rm N}$, we obtain the second equality in Eq. (2.43). The term (2.43) combined with the first term on the RHS of Eq. (2.38) gives a finite result. We therefore write

$$\delta E_{2D} - i \int \frac{d^4k}{(2\pi)^4} \text{Tr}(S_{0D}(\delta \tilde{m}_N - \tilde{k}(Z_N - 1))) = E_{(1)}^{\text{ex}} + E_{(2)}^{\text{ex}}$$
 (2.45a)

with the "exchange energies"

$$E_{(1)}^{\text{ex}} = \frac{g^2}{2} \int \frac{d^4k}{(2\pi)^4} \int \frac{d^4q}{(2\pi)^4} \Delta_{\text{of}}(k) \operatorname{Tr}(S_{0D}(q) S_{0D}(k+q)) + \frac{g_{\omega}^2}{2} \int \frac{d^4k}{(2\pi)^4} \int \frac{d^4q}{(2\pi)^4} \Delta_{\text{of}}(k) \operatorname{Tr}(\gamma_{\mu} S_{0D}(q) \gamma^{\mu} S_{0D}(k+q))$$
(2.45b)

$$E_{(2)}^{\text{ex}} = -i \, \Sigma_{\text{NF}} |_{\tilde{k} = \tilde{m}_{\text{N}}} \int \frac{d^4k}{(2\pi)^4} \, \text{Tr} \, S_{\text{0D}}$$
 (2.45c)

with

$$\Sigma_{\rm NF}|_{\tilde{k}=\tilde{m}_{\rm N}} = \overline{\Sigma}_{\rm NF}|_{\tilde{k}=\tilde{m}_{\rm N}} - \frac{\tilde{m}_{\rm N}}{m_{\rm N}} \, \overline{\Sigma}_{\rm Nf}|_{\tilde{k}=m_{\rm N}}.$$
(2.45d)

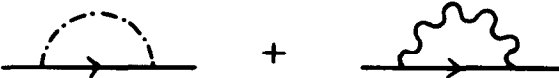


Fig. 3. Diagrams for the Feynman part of the nucleon self-energy (2.44). Here the full line denotes the propagator S_{0F} , and the dashed-dotted and wavy lines are for the free σ and ω propagators, respectively.

From the general relation $\Sigma_{NF} = \overline{\Sigma}_{NF} + \delta \tilde{m}_N - \tilde{k}(Z_N - 1)$ between the renormalized and the unrenormalized nucleon self-energies it is seen that (2.45d) is indeed the renormalized self-energy at $\tilde{k} = \tilde{m}_N$ and hence is finite.

Let us now add together all the remaining divergent terms, i.e., the second term in (2.38), the terms (2.39b)–(2.39d) and (2.42e), (2.42f). The second term in (2.38) combined with (2.39d) gives

$$-i \int \frac{d^4k}{(2\pi)^4} \text{Tr}(S_{0F}(\delta \tilde{m}_N - \tilde{m}_N(Z_N - 1)) + (2.39d) = \frac{1}{2\pi^2} \frac{\bar{\Sigma}_{Nf}}{m_N} \bigg|_{b = m_N} C, \quad (2.46a)$$

where the constant C is given by

$$C = \tilde{m}_{N}^{4} \ln \frac{\tilde{m}_{N}^{2}}{m_{N}^{2}} - m_{N}^{2} \delta_{N} - \frac{3}{2} \delta_{N}^{2}.$$
 (2.46b)

Now adding together the divergent terms listed above we get

$$(2.46a) + (2.39b) + (2.39c) + (2.42e) + (2.42f) = E_{(3)}^{ex} + E^{V}$$
 (2.47a)

with

$$E_{(3)}^{\text{ex}} = \frac{i}{2} \int \frac{d^4k}{(2\pi)^4} \left(\Pi_{\sigma F}^{(-2)} \Delta_{\sigma f} - 3\Pi_{TF}^{(-2)} \Delta_{\omega f} \right) + \frac{1}{2\pi^2} \frac{\bar{\Sigma}_{Nf}}{m_N} \bigg|_{p = m_N} C$$
 (2.47b)

$$E^{V} = \frac{i}{4} \int \frac{d^{4}k}{(2\pi)^{4}} \left((2\delta_{\sigma} \Pi_{\sigma F}^{(-1)} + [\Pi_{\sigma F}^{2}]^{(-1)}) \Delta_{\sigma f}^{2} + 3[\Pi_{TF}^{2}]^{(-1)} \Delta_{\omega f}^{2} \right). \quad (2.47c)$$

Here $\Pi^{(-2)}(\Pi^{(-1)})$ denotes the value of the polarization Π after the first two (one) powers in an expansion around $\tilde{m}_N^2 = m_N^2$ have been subtracted,

$$\Pi_{iF}^{(-1)} = \Pi_{iF} - \delta_{N} \Sigma_{iF}'$$
 (2.48a)

$$\Pi_{iF}^{(-2)} = \Pi_{iF} - \delta_{N} \Sigma_{iF}' - \frac{1}{2} \delta_{N}^{2} \Sigma_{iF}''$$
 (2.48b)

with $i = \sigma$ or T. In (2.47c) we further introduced the notation

$$[\Pi_{iF}^{2}]^{(-1)} = \Pi_{iF}^{2} - (\delta_{N} \Sigma_{iF}')^{2}.$$
 (2.48c)

In the next section it will be shown that the expressions (2.47b) and (2.47c) are finite.

We can now write down the final expression for the energy density (2.22). We have to add Eqs. (2.41a), (2.39a), (2.42b), (2.42c), (2.45a), and (2.47a) and obtain

$$E = E^{\text{QCL}} + E_{(1)}^{\text{ex}} + E_{(2)}^{\text{ex}} + E_{(3)}^{\text{ex}} + E^{\text{V}} + E_{\text{N}}^{\text{C}} + E_{\text{L}}^{\text{C}} + E_{\text{L}}^{\text{C}}.$$
(2.49)

Here the quasiclassical contribution is given by

$$E^{\text{QLC}} = U + 4 \int \frac{d^3k}{(2\pi)^3} \tilde{E}_k n(k) + g_\omega \tilde{w}^\circ \rho$$
 (2.50)

with U from Eq. (2.13). The three "exchange energies" E^{ex} , being of second order in the coupling constants, are given by (2.45b), (2.45c), and (2.47b), the fourth-order term E^{V} is given by (2.47c), and the "correlation energies" E^{C} are given by (2.41b), (2.42b), and (2.42c).

2.3. Polarization Insertions and Stability Conditions

Let us inspect more closely some of the loop terms in (2.49). Our intention here is, first, to show the finiteness of (2.49), second, to derive certain stability conditions which will restrict the choice of the parameters, and, finally, to discuss the signs of the various terms.

(a) Exchange terms and the fourth-order term $E^{\rm V}$. The three "exchange energies" $E_{(i)}^{\rm ex}$, i=1,2,3, in Eq. (2.49) can be represented graphically by Fig. 4. According to our derivation, $E_{(1)}^{\rm ex}$ is due to the combination $S_{\rm 0D}S_{\rm 0D}$, $E_{(2)}^{\rm ex}$ due to $S_{\rm 0D}S_{\rm 0F}$, and $E_{(3)}^{\rm ex}$ due to $S_{\rm 0F}S_{\rm 0F}$ in the diagrams of Fig. 4. The numerical evaluation of the traditional Fock term $E_{(1)}^{\rm ex}$ according to (2.45b) presents no difficulties [2]. As expected from the nonrelativistic picture, the σ meson contributes repulsion here while the ω meson gives an attraction. The term $E_{(2)}^{\rm ex}$ of (2.45c) is due to the shift $m_{\rm N} \to \tilde{m}_{\rm N}$ of the nucleon mass. Its evaluation requires the renormalized Feynman part of the nucleon self-energy $\Sigma_{\rm NF}$. According to our definition (2.44), this quantity involves the full meson propagators in free space. As we will discuss later in connection with the introduction of cutoff functions, however, in the actual calculations we will neglect the free space meson polarizations. In this approximation, the unrenormalized nucleon self-energy of (2.44) becomes

$$16\pi^{2}\bar{\Sigma}_{NF}(p) = g^{2}(\tilde{m}_{N}F_{\sigma}^{(0)}(\tilde{p}^{2},\tilde{m}_{N}^{2}) + \tilde{p}F_{\sigma}^{(1)}(\tilde{p}^{2},\tilde{m}_{N}^{2})) + g_{\omega}^{2}(-4\tilde{m}_{N}F_{\omega}^{(0)}(\tilde{p}^{2},\tilde{m}_{N}^{2}) + 2\tilde{p}F_{\omega}^{(1)}(\tilde{p}^{2},\tilde{m}_{N}^{2}))$$
(2.51a)

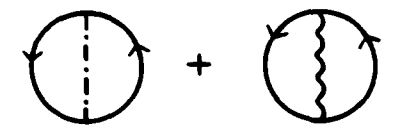


Fig. 4. Graphical representation of the exchange energies in Eq. (2.49). The full line stands for the Hartree propagator, and the dashed-dotted and wavy lines for the free σ and ω meson propagators, respectively. Counterterm contributions are not indicated in the figure.

with

$$F_{\alpha}^{(a)}(p^{2}, m^{2}) = -(\frac{1}{2})^{a} \Gamma(2 - \frac{n}{2}) + f_{\alpha}^{(a)}(p^{2}, m^{2}),$$

$$f_{\alpha}^{(a)}(p^{2}, m^{2}) = \int_{0}^{1} dx \ x^{a} \ln(m^{2} + (m_{\alpha}^{2} - m^{2}) \ x - p^{2} x (1 - x)) \qquad (2.51b)$$

$$(\alpha = \sigma, \omega; a = 0, 1).$$

The renormalized self-energy at $\tilde{p} = \tilde{m}_{N}$ is then found from (2.45d) as

$$16\pi^{2}\Sigma_{NF}|_{\tilde{\theta}=\tilde{m}_{0}} = g^{2}\tilde{m}_{N}(f_{\sigma}^{(0)} + f_{\sigma}^{(1)}) - 2g_{\omega}^{2}\tilde{m}_{N}(2f_{\omega}^{(0)} - f_{\omega}^{(1)})$$
 (2.52a)

with

$$f_{\alpha}^{(a)} = f_{\alpha}^{(a)}(\tilde{m}_{N}^{2}, \tilde{m}_{N}^{2}) - f_{\alpha}^{(a)}(m_{N}^{2}, m_{N}^{2})$$

$$= \int_{0}^{1} dx \, x^{a} \ln \frac{\tilde{m}_{N}^{2}(1-x)^{2} + m_{\alpha}^{2}x}{m_{N}^{2}(1-x)^{2} + m_{\alpha}^{2}x}.$$
(2.52b)

It is seen that $\sigma(\omega)$ contributes attraction (repulsion) to (2.52a) and hence also to the term $E_{(2)}^{\text{ex}}$ of (2.45c).

The evaluation of the next two terms $E_{(3)}^{\rm ex}$ and $E^{\rm v}$ in (2.49) requires the Feynman parts of the meson self-energies. These are obtained by replacing $S_0 \to S_{0\rm F}$ in (2.29a), (2.29b):

$$16\pi^{2}\Sigma_{\sigma F} = 4g^{2}(k^{2} - 4\tilde{m}_{N}^{2}) \int_{0}^{1} dx \ln \frac{\tilde{m}_{N}^{2} - k^{2}x(1 - x)}{m_{N}^{2}}$$
$$-8g^{2}\tilde{m}_{N}^{2} \ln \frac{\tilde{m}_{N}^{2}}{m_{N}^{2}} + 8g^{2}(\tilde{m}_{N}^{2} - m_{N}^{2})$$
(2.53a)

$$16\pi^2 \Sigma_{\rm TF} = 16g_{\omega}^2 k^2 \int_0^1 dx \ x(1-x) \ln \frac{\tilde{m}_{\rm N}^2 - k^2 x(1-x)}{m_{\rm N}^2}.$$
 (2.53b)

For $k^2 = 0$ and \tilde{m}_N/m_N between 0.4 and 1, (2.53a) gives a large positive contribution, which will strongly influence our later discussions. The polarizations Π_F introduced in (2.32) are obtained from the above expressions by subtracting the free space values ($\tilde{m}_N = m_N$).

In order to show that the expressions (2.47b), (2.47c) are finite, we need the asymptotic forms of the polarizations for large k^2 . We obtain $(i = \sigma, T)$

$$\Pi_{iF} \propto \log k^2 + O[\log k^2/k^2]$$
 (2.54a)

$$\Pi_{iF}^{(-1)} \propto \frac{\log k^2}{k^2} + O[1/k^2]$$
(2.54b)

$$[\Pi_{iF}^{2}]^{(-1)} \propto \frac{\log k^{2}}{k^{2}} + O[1/k^{2}]$$
 (2.54c)

$$\Pi_{\sigma F}^{(-2)} = -\frac{g^2}{\pi^2} \frac{3}{2} \frac{1}{k^2} C + O[1/k^4]$$
 (2.54d)

$$\Pi_{\rm TF}^{(-2)} = \frac{g_{\omega}^2}{\pi^2} \frac{1}{k^2} C + O[1/k^4],$$
(2.54e)

where C has been given in (2.46b). Due to (2.54b), (2.54c), E^{V} of (2.47c) is finite. From (2.54d), (2.54e) it follows that the divergence of the first term in (2.47b) is given by

$$\frac{1}{16\pi^2} \frac{C}{2\pi^2} \left(\frac{3}{2} g^2 - 3g_{\omega}^2 \right) \Gamma(2 - \frac{n}{2}).$$

This divergence is cancelled by the second term of (2.47b), as can be seen from the form of the unrenormalized nucleon self-energy in free space, obtained by setting $\tilde{m}_N = m_N$ in (2.51). This shows that also the contribution (2.47b) is finite.

The integrals in (2.47b), (2.47c) are calculated numerically by performing a Wick rotation $(k^2 \rightarrow l^2 = -k_0^2 - \mathbf{k}^2)$; we will use a hat on a quantity to characterize its Wick rotated expression). We obtain, leaving out the free space meson self-energies,

$$16\pi^{2}E_{(3)}^{\text{ex}} = \int_{0}^{\infty} l^{3} dl \left(\frac{\hat{\Pi}_{\sigma F}^{(-2)}}{l^{2} + m_{\sigma}^{2}} + 3 \frac{\hat{\Pi}_{TF}^{(-2)}}{l^{2} + m_{\omega}^{2}} \right)$$
(2.55a)

+
$$\frac{C}{2\pi^2}$$
[$g^2(f_{\sigma}^{(0)}(m_N^2, m_N^2) + f_{\sigma}^{(1)}(m_N^2, m_N^2))$

+
$$g_{\omega}^{2}(-4f_{\omega}^{(0)}(m_{N}^{2}, m_{N}^{2}) + 2f_{\omega}^{(1)}(m_{N}^{2}, m_{N}^{2}))]$$
 (2.55b)

$$-\frac{C}{2\pi^2}\Gamma(2-\frac{n}{2})\left(\frac{3}{2}g^2-3g_{\omega}^2\right)$$
 (2.55c)

$$16\pi^{2}E^{V} = -\frac{1}{2} \int_{0}^{\infty} l^{3} dl \left(\frac{2\delta_{\sigma} \hat{\Pi}_{\sigma F}^{(-1)} + \left[\hat{\Pi}_{\sigma F}^{2}\right]^{(-1)}}{(l^{2} + m_{\sigma}^{2})^{2}} + 3 \frac{\left[\hat{\Pi}_{TF}^{2}\right]^{(-1)}}{(l^{2} + m_{\omega}^{2})^{2}} \right). \quad (2.56)$$

If one does not introduce a cutoff function, one should make use of the asymptotic expansion given in (2.54d), (2.54e) to subtract a suitable function from the integrand in (2.55a) and add it again, thereby cancelling the divergent term (2.55c) analytically. (For example, a possible choice concerning the σ meson contributions in (2.55) would be the function $3Cg^2/2\pi^2 \cdot 1/((l^2 + \mu^2)(l^2 + m_\sigma^2))$, where μ is an arbitrary mass.) However, as we will explain later, we will evertually introduce a cutoff function, which enables us to calculate the two terms (2.55a), (2.55b) separately. We will then see (in Section 3.2) that the contribution of the σ meson to $\overline{\mathcal{L}}_{Nf}$ is negative and hence the σ meson part of the term (2.55b) is positive. (Note that C < 0.) The σ meson term in (2.55a) cancels part of this repulsive contribution,

which can be understood from the fact that $\hat{\Pi}_{\sigma F}^{(-2)} < 0$ for small l^2 . For the ω meson the situation is just reversed; i.e., the ω meson part of the sum (2.55a) + (2.55b) gives attraction.

The fourth-order term E^{V} of Eq. (2.56) will turn out to depend very strongly on the assumed value for m_{σ} . We have $\delta_{\sigma} < 0$, and also both $\hat{H}_{\sigma F}^{(-1)}$ and $[\hat{H}_{\sigma F}^{2}]^{(-1)}$ are negative for small l^{2} . Roughly speaking, for $m_{\sigma} \lesssim 1.2$ GeV one gets a repulsive contribution from (2.56). For higher m_{σ} , however, the mass shift δ_{σ} becomes increasingly important and E^{V} turns into an attractive contribution. The ω meson term in (2.56) will be seen to be small compared with the σ contribution.

(b) Correlation energies. Next we turn to the correlation energies in Eq. (2.49). For the nucleonic contribution we have the simple Hartree expression (2.41b), which can be given analytically as [3, 4]

$$E_{N}^{C} = -\frac{m_{N}^{4}}{8\pi^{2}} F(y_{N}); \qquad y_{N} = \left(\frac{\tilde{m}_{N}}{m_{N}}\right)^{2},$$

$$F(y) = y^{2} \ln y - \frac{3}{2} (y^{2} - 1) + 2(y - 1). \tag{2.57}$$

For $y_N < 1$ we have $E_N^C > 0$. The positive sign is easily understood from the fact that E_N^C is nothing but the energy of the Dirac sea minus the vacuum value

$$E_{\rm N}^{\ C} = -4 \int \frac{d^3k}{(2\pi)^3} \left(\sqrt{\tilde{m}_{\rm N}^2 + \mathbf{k}^2} - \sqrt{m_{\rm N}^2 + \mathbf{k}^2} \right) + \text{counterterms.}$$
 (2.58)

The longitudinal and transverse correlation energies have been given in (2.42b), (2.42c). For their numerical evaluation we will perform a Wick rotation $(k_0 \rightarrow \omega = ik_0)$. If we include both the explicitly density dependent and the Feynman parts in the meson propagators, the imaginary parts of the self-energies have the correct (negative) sign, which implies that the propagators have neither zeros nor poles for complex k_0^2 [8]. This leaves the possibility of real (physical) poles and poles on the imaginary k_0 axis (tachyon poles). For the system to be stable the latter ones have to be avoided, which imposes the "stability conditions"

$$\hat{\varepsilon}_{L}(l) > 0 \tag{2.59a}$$

$$\hat{\varepsilon}_{\mathrm{T}}(l) > 0 \tag{2.59b}$$

for all values of the Euclidean four vector $l = (\omega, \mathbf{k})$. An instability of the system occurs if a pole at $k_0^2 > 0$ passes the origin in the complex k_0^2 plane and moves to the tachyon region $k_0^2 < 0$ [8]. Hence, in practice it is sufficient to impose the conditions (2.59) for $\omega = 0$. We should note that our above discussion holds only if the Feynman parts of the polarizations are included. In the widely used approximation of including only the density parts, the propagators can have poles at complex k_0^2 , and one obtains different results when the Feynman parts are neglected before or

after the Wick rotation. In the numerical calculations to be discussed in Section 3 we will investigate the approximation of neglecting the Feynman parts in the Wick rotated expressions.

Let us discuss the low momentum limits of (2.59), where Eq. (2.59a) imposes a rather strong condition on the choice of the parameters. We have for $l = (\omega, \mathbf{k}) \to 0$ (see Appendix B)

$$\hat{\varepsilon}_{L}(0) = \frac{m_{\sigma}^{*2} + \Sigma_{\sigma F}(0)}{m_{\sigma}^{2}} \frac{m_{\omega}^{*2}}{m_{\omega}^{2}}$$
(2.60a)

$$\hat{\varepsilon}_{L}^{(st)}(0) = \frac{m_{\sigma}^{*2} + \Sigma_{\sigma F}(0)}{m_{\sigma}^{2}} (1 + F_{0}^{(H)}). \tag{2.60b}$$

Here we used the notations

$$m_{\sigma}^{*2} = \tilde{m}_{\sigma}^{2} + \Sigma_{\sigma D}(0) = \tilde{m}_{\sigma}^{2} + 4g^{2} \int \frac{d^{3}k}{(2\pi)^{3}} \frac{\mathbf{k}^{2}}{\tilde{E}_{k}^{3}} n(k)$$
 (2.61a)

$$16\pi^{2}\Sigma_{\sigma F}(0) = 8g^{2}\left(\tilde{m}_{N}^{2} - m_{N}^{2} - 3\tilde{m}_{N}^{2} \ln \frac{\tilde{m}_{N}^{2}}{m_{N}^{2}}\right)$$
(2.61b)

$$m_{\omega}^{*2} = m_{\omega}^{2} + \Pi_{TD}(0) = m_{\omega}^{2} + g_{\omega}^{2} \frac{\rho}{E_{r}}$$
 (2.61c)

$$F_0^{(H)} = N_F^{(H)} \left(\frac{g_\omega^2}{m_\omega^2} - g^2 \left(\frac{\tilde{m}}{E_F} \right)^2 \frac{1}{m_\sigma^{*2} + \Sigma_{\sigma F}(0)} \right). \tag{2.61d}$$

In the above formulae, the limits $k \to 0$ of a quantity A(k) are denoted as $A(0) = \lim_{k_0 \to 0} \lim_{k_0 \to 0} A(k)$ and $A^{(st)}(0) = \lim_{k_0 \to 0} \lim_{k_0 \to 0} A(k)$. (The two limits do not commute, since the particle hole excitations vanish in the former but not in the latter limit.) We further used $E_F = \sqrt{p_F^2 + \tilde{m}_N^2}$, and $N_F^{(H)} = 2p_F E_F/\pi^2$ is the density of states at the Fermi surface in the Hartree approximation. The mass parameters m_σ^{*2} or $(m_\sigma^{*2} + \Sigma_{\sigma F}(0))$ are the "self consistent" σ mass parameters in a one-loop calculation; i.e., they agree with the quantity $-\Delta_\sigma^{-1}(0)$ of (2.23b) if the energy density E equals E^{QCL} or $E^{(H)} = E^{QCL} + E_N^C$ (see Eq. (2.49)), respectively. Similarly, m_ω^{*2} is the self-consistent ω meson mass parameter in a one loop calculation [4]. Finally, $F_0^{(H)}$ is the dimensionless l = 0 Landau-Migdal parameter calculated from the one-loop energy density $E^{(H)}$ in the usual way [4, 12]. We see that the condition (2.59a) implies

$$m_{\sigma}^{*2} + \Sigma_{\sigma F}(0) > 0$$
 (2.62a)

$$1 + F_0^{(H)} > 0. (2.62b)$$

The conditions (2.62) are necessary in order that the meson propagators are free of Tachyon poles at low momenta, i.e., in order that the energy density is real. They do not guarantee the stability of the two loop energy density (2.49) with respect to

variations in \tilde{v} for fixed density, nor with respect to variations in the density. Since we calculated these meson propagators in the one loop approximation retaining only the nucleon loop, the conditions (2.62) derived above agree with the following stability conditions to be imposed on the Hartree energy density: $\partial^2 E^{(H)}/\partial \tilde{v}^2 > 0$ for fixed ρ , and $\partial^2 E^{(H)}/\partial \rho^2 > 0$ at the extremum of $E^{(H)}(\rho)$. We will come back to this correspondence in the next section. Eq. (2.59b) for $l \to 0$ imposes no further conditions. We have $\hat{\varepsilon}_T(0) = m_\omega^{*2}/m_\omega^2$ and $\hat{\varepsilon}_T^{(si)}(0) = 1$.

Turning now to the high momentum region, we note that the $k^2 \ln(-k^2)$ behaviour of the polarizations (2.53) leads to zeros of the polarizabilities at space like momenta ($k^2 < 0$). In particular, the meson propagators (2.34) in free space have tachyon poles. This problem occurs also for the photon propagator in Q.E.D. One possibility to avoid the tachyon pole has been proposed in Ref. [13] and consists in introducing the chain approximation in the spectral function of the Källén-Lehmann representation. The resulting propagators are different from (2.34) and free of Tachyon poles. In this work, however, we will avoid the tachyon poles caused by the Feynman parts of the polarizations by introducing a meson-nucleon vertex form factor. This point will be further discussed in the next section. Without the introduction of vertex form factors there is also the possibility that for high density and/or small values of \tilde{m}_N the density part of the transverse polarization $\Pi_{\rm TD}$ causes $\hat{\varepsilon}_{\rm T}$ to become negative. For example, for $g_{\omega} = 15$, $\rho = 0.5$ fm⁻³, and $\tilde{m}_{\rm N}/m_{\rm N} = 0.6$, $\hat{\Pi}_{\rm TD}/(l^2 + m_{\omega}^2)$ becomes less than -1 at $\omega \approx 0$, $|\mathbf{k}| \approx 450$ MeV. The reason for this is very similar to that for pion condensation: The transverse part of the nonrelativistic ω meson exchange potential contains a δ function piece which is attractive in this channel. Since this instability occurs at rather high values of $|\mathbf{k}|$, it can, unlike the case of pion condensation, be avoided by introducing a mesonnucleon cutoff function. Another possibility is to introduce a phenomenological two-body interaction (nonrelativistically usually written in momentum space as $4\pi f^2/m_\pi^2 g_s(\mathbf{\sigma}_1 \cdot \mathbf{\sigma}_2)$, which simulates the effects of exchange and short range correlations. For example, the choice $g_s = 0.1$ eliminates the singularity mentioned above, as does also a dipole form factor with $\Lambda = 1$ GeV.

Returning now to the correlation energies (2.42b), (2.42c), a Wick rotation gives the following expressions which will be used for the numerical calculations:

$$E_{L}{}^{C} = \frac{1}{4\pi^{3}} \int_{0}^{\infty} l^{3} dl \int_{0}^{\pi/2} \sin^{2}\theta d\theta \left\{ \ln \hat{\varepsilon}_{L} - \frac{\hat{\Pi}_{\sigma}}{l^{2} + m_{\sigma}^{2}} + \frac{\hat{\Pi}_{L}}{l^{2} + m_{\omega}^{2}} + \frac{1}{2} \left(\frac{\delta_{\sigma} + \hat{\Pi}_{\sigma F}}{l^{2} + m_{\sigma}^{2}} \right)^{2} + \frac{1}{2} \left(\frac{\hat{\Pi}_{LF}}{l^{2} + m_{\omega}^{2}} \right)^{2} \right\}$$

$$E_{T}{}^{C} = \frac{1}{2\pi^{3}} \int_{0}^{\infty} l^{3} dl \int_{0}^{\pi/2} \sin^{2}\theta d\theta \left\{ \ln \hat{\varepsilon}_{T} - \frac{\hat{\Pi}_{T}}{l^{2} + m_{\omega}^{2}} + \frac{1}{2} \left(\frac{\hat{\Pi}_{TF}}{l^{2} + m_{\omega}^{2}} \right)^{2} \right\}.$$
 (2.63b)

Here the Wick rotated polarizabilities are given by

$$\hat{\varepsilon}_{L} = \left(1 + \frac{\hat{\Pi}_{\sigma}}{l^{2} + m_{\sigma}^{2}}\right) \left(1 - \frac{\hat{\Pi}_{L}}{l^{2} + m_{\omega}^{2}}\right) + \frac{\hat{\Pi}_{M}^{2}}{(l^{2} + m_{\sigma}^{2})(l^{2} + m_{\omega}^{2})}$$
(2.64a)

$$\hat{\varepsilon}_{\rm T} = 1 - \frac{\hat{\Pi}_{\rm T}}{l^2 + m_{\rm co}^2}.$$
 (2.64b)

Here $\tan \theta = |\mathbf{k}|/\omega$, and we again approximated the free space meson propagators by their lowest order forms. If all self-energy pieces in (2.63a) are neglected and only the mass shift δ_{σ} is retained, $E_{\rm L}^{C}$ is equivalent to the "zero-point oscillation" energy of the σ field discussed in the Introduction,

$$E_{\rm L}^{\ C} \to \frac{1}{2} \int \frac{d^3k}{(2\pi)^3} \left(\sqrt{\tilde{m}_{\sigma}^2 + \mathbf{k}^2} - \sqrt{m_{\sigma}^2 + \mathbf{k}^2} \right) + \text{counterterms},$$
 (2.65)

which is attractive and known to cancel large parts of the nucleonic contribution (2.58) [3]. The effect of the density part of the σ polarization $\hat{\Pi}_{\sigma D}$ in (2.63a) has been roughly estimated in previous calculations [1, 3, 4] by replacing $\hat{m}_{\sigma}^{2} \rightarrow m_{\sigma}^{*2}$ in (2.65), where m_{σ}^{*2} is given by Eq. (2.61a). Note, however, that in the opposite limit of $\omega \rightarrow 0$ followed by $|\mathbf{k}| \rightarrow 0$, $\hat{\Pi}_{\sigma D}$ is negative and very large due to the attractive nature of the particle hole interaction mediated by σ meson exchange. Physically we expect that this effect, which is partially cancelled due to the presence of the ω meson (i.e., the mixing term in (2.64a)), will enlarge the attractive contribution due to $E_{\rm L}^{C}$. On the other hand, the Feynman part $\hat{\Pi}_{\sigma F}$ is positive and very large at small momenta and, as we shall see, can even change $E_{\rm L}^{C}$ into a repulsive contribution. We will come to this point later. The contribution due to $E_{\rm T}^{C}$ will turn out to be small in our subsequent calculations.

3. RESULTS AND DISCUSSIONS

In this section we will show the results for the binding energy per nucleon based on the expression (2.49) and analyze them in detail. This will be done in two steps: First, in Section 3.1, we neglect the Feynman parts of the meson polarizations (2.29); i.e., the polarizations in this case include the familiar particle-hole excitations and the Pauli principle corrections to the $N\bar{N}$ excitations. Second, in Section 3.2, the Feynman parts will be re-included. Our conclusion will be that we cannot achieve a satisfactory description of nuclear matter within the framework discussed so far. In particular, if the Feynman parts of the meson polarizations are included the saturation of the binding energy is lost. After analyzing the situation we will see that, once the vacuum fluctuations are considered, the meson loop contributions to the meson polarizations (see Fig. 1b, 2b) should be taken into account simultaneously with the nucleon loops. Therefore, in Section 3.3, we will estimate the influence of these meson loops on the correlation energies. This modification of the correlation energies leads to a recovery of the saturation.

In all subsequent calculations we fix g=10 due to reasons discussed earlier. We further use $m_N=939$ MeV, v=93.9 MeV due to (2.4a), $m_\omega=783$ MeV, and in (2.4b) and (2.13) we use $m_\pi=140$ MeV. The free parameters are m_σ and g_ω .

3.1. Feynman Parts of Polarizations Neglected

Here we include only the pieces $\Sigma_{\sigma D}$ and $\Sigma_{\omega D}$ of Eq. (2.29). Their analytical expressions are given in Ref. [14], and in Appendix C we give the corresponding formulae after Wick rotation. No meson-nucleon vertex form factors will be included in the present subsection.

First we discuss the stability conditions (2.62) for $\Sigma_{\sigma F} = 0$. To satisfy (2.62a) makes no essential difficulties, but Eq. (2.62b) imposes severe restrictions. For normal densities m_{σ}^{*2} decreases as \tilde{v}/v deviates from unity towards smaller values, and accordingly the parameter $F_0^{(H)}$ of Eq. (2.61d) becomes more negative. For example, choosing $g_{\omega} = g = 10$ and $m_{\sigma} = 1$ GeV, the possible values of \tilde{v}/v are restricted to $\tilde{v}/v \gtrsim 0.8$ for all densities $\rho \lesssim 0.4$ fm⁻³. For higher densities this lower limit decreases gradually but slowly. From this and Eq. (2.61d) we see that we need rather high values of g_{ω} and/or m_{σ} in order to have some freedom in varying \tilde{v} when minimizing the energy density with respect to \tilde{v} for fixed ρ . For medium and high densities ($\rho \gtrsim 0.15$ fm⁻³), there is also an allowed region of small \tilde{v}/v .

The Wick-rotated polarizabilities $\hat{\varepsilon}_L$ and $\hat{\varepsilon}_T$ are shown in Fig. 5 for a small value of ω ($\omega = 20$ MeV) as a function of $|\mathbf{k}|$. The density is chosen as $\rho = 0.15$ fm $^{-3}$, and $\tilde{v}/v = 0.85$. The other parameters are

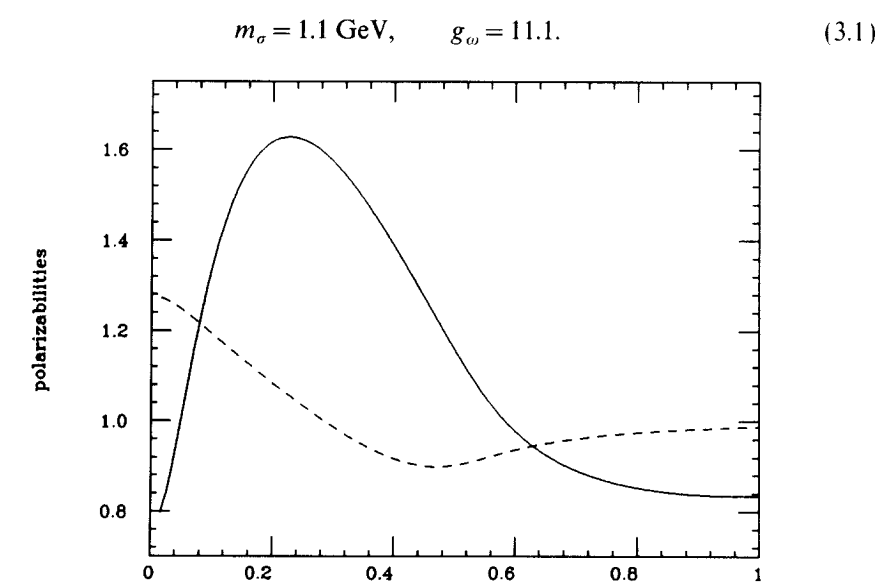


Fig. 5. The Wick rotated longitudinal (full line) and transverse (dashed line) polarizabilities of Eq. (2.64) without the Feynman parts in the meson self-energies. The case shown here refers to $\rho = 0.15 \text{ fm}^{-3}$, $\tilde{v}/v = 0.85$, $\omega = 20 \text{ MeV}$.

k [GeV]

We see that for medium values of the three momentum $\hat{\varepsilon}_L$ deviates very much from unity, in contrast to $\hat{\varepsilon}_T$. The value of $\hat{\varepsilon}_L$ at $|\mathbf{k}| = 0$ is approximately given by (2.60a). The sudden increase of $\hat{\varepsilon}_L$ at low $|\mathbf{k}|$ is due to the particle-hole excitations in the mixing part $\hat{\Pi}_M^2$ of Eq. (2.64a). (Note that the particle-hole excitation processes vanish for $|\mathbf{k}| \to 0$, $\omega \neq 0$.) The contributions of particle-hole excitations in $\hat{\Pi}_\sigma$ are negative for small ω , but they are overwhelmed by the mixing term due to the large g_ω . This shows the important role of the σ - ω mixing in order to satisfy the condition (2.59a). The sharp peak of $\hat{\varepsilon}_L$ shown in Fig. 5 persists only for low ω .

The results for the binding energy per nucleon are shown in Fig. 6a. Here, in addition to the choice (3.1), we show the results obtained by slight changes of g_{ω} . The nucleon effective mass is shown in Fig. 6b. The prominent features of this calculation are, first, that for densities $\rho \gtrsim 0.16$ fm $^{-3}$ we do not find a minimum of the energy density as a function of \tilde{v} and hence no stable nuclear matter state, and, second, that for certain parameters nuclear matter saturates at about half of the normal nuclear matter density with a rather low binding energy. We found that this situation cannot be improved by choosing a different parameter set or by introducing meson–nucleon vertex form factors. The following discussion analyzes the results of Fig. 6.

Figure 7 shows the binding energy per nucleon for some fixed densities as a function of \tilde{v}/v . For $\rho \lesssim 0.16$ fm⁻³ each curve shows a minimum, and the corresponding "physical" values \tilde{v}_0 and $E_{\rm B}/A$ have been used to draw Fig. 6. According to Eq. (2.23a), \tilde{v}_0 is a solution of the equation

$$\Sigma_{\pi}(0) = -\left(\tilde{m}_{\pi}^{2} - \frac{c}{\tilde{v}}\right),\tag{3.2a}$$

and the curvature at $\tilde{v} = \tilde{v}_0$ is given by

$$M_{\sigma}^{*2} = \tilde{m}_{\sigma}^{2} + \Sigma_{\sigma}(0).$$
 (3.2b)

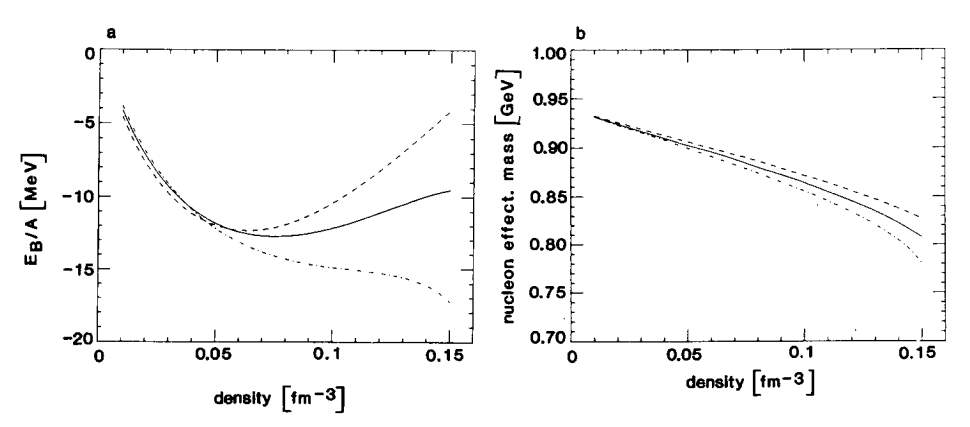


Fig. 6. Binding energy per nucleon (a) and the nucleon effective mass (b) calculated by neglecting the Feynman parts in the meson self-energies. The three lines refer to different values for g_{ω} : $g_{\omega} = 10.9$ (dashed-dotted line), $g_{\omega} = 11.1$ (full line), $g_{\omega} = 11.3$ (dashed line). The σ mass is $m_{\sigma} = 1.1$ GeV.

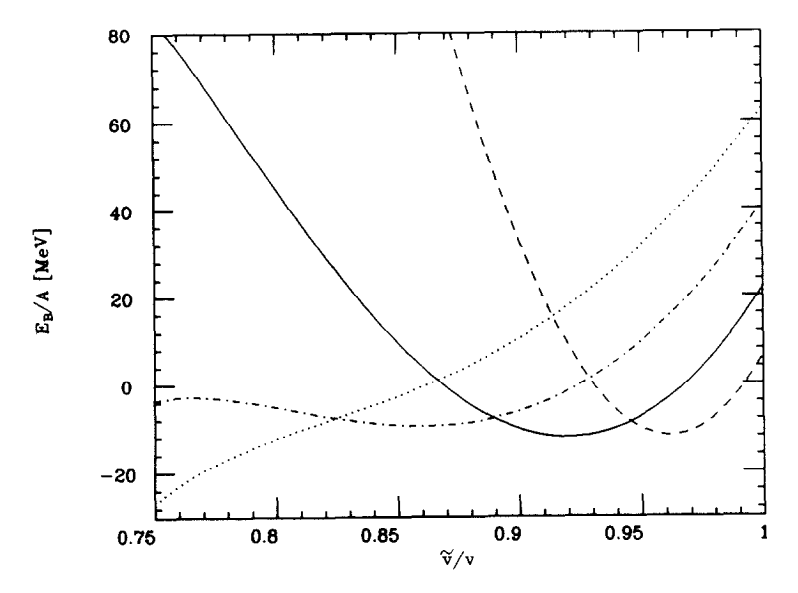


Fig. 7. Binding energy per nucleon as a function of \bar{v}/v for various densities: 0.05 fm⁻³ (dashed line), 0.1 fm⁻³ (full line), 0.15 fm⁻³ (dashed-dotted line), 0.2 fm⁻³ (dotted line). The case refers to the full line of Fig. 6a.

As shown in Appendix A, the two loop self-energies in these expressions are given by

$$\Sigma_{\alpha} = \Sigma_{\alpha D} + \Sigma_{\alpha F} + \Sigma_{\alpha, \text{mes}} + \delta \Sigma_{\alpha} \qquad (\alpha = \sigma, \pi), \tag{3.3}$$

where the first two terms constitute the nucleonic contribution (2.29) shown in Figs. 1a, 2a, the third term is the meson loop contribution of Figs. 1b, 2b, and $\delta \Sigma_{\pi}$ is the contribution of the vertex and self-energy corrections to the nucleon loop diagrams, see Figs. 1c, 2c. It is evident from Fig. 7 that for $\rho \approx 0.16$ fm⁻³ the mass parameter M_a^{*2} becomes zero, and beyond this density Eq. (3.2a) no longer has a solution. This situation, which is very similar to the one observed already in the quasiclassical approximation [4], is shown in more detail in Fig. 8, which illustrates Eqs. (3.2) for a fixed density $\rho = 0.15 \, \mathrm{fm}^{-3}$. The dashed double-dotted line in Fig. 8a shows the right-hand side of Eq. (3.2a), and the full line the two-loop pion self-energy $\Sigma_{\pi}(0)$. There are two solutions to Eq. (3.2a), one corresponding to a minimum of the energy density and the other to a maximum, see also Fig. 7. If we increase the density further, the two solutions coalesce, and beyond that density the full line in Fig. 8a lies above the dashed double-dotted one such that Eq. (3.2a) has no solution. The quantity M_{σ}^{*2} of Eq. (3.2b) is shown by the full line in Fig. 8b. For $\tilde{v} = \tilde{v}_0$ we still have $M_{\sigma}^* = 670$ MeV, but for higher densities M_{σ}^* vanishes at the physical point \tilde{v}_0 . The same quantities are shown as functions of the density in Fig. 9. Since Eq. (3.2a) is satisfied at every density, the dashed double-dotted and

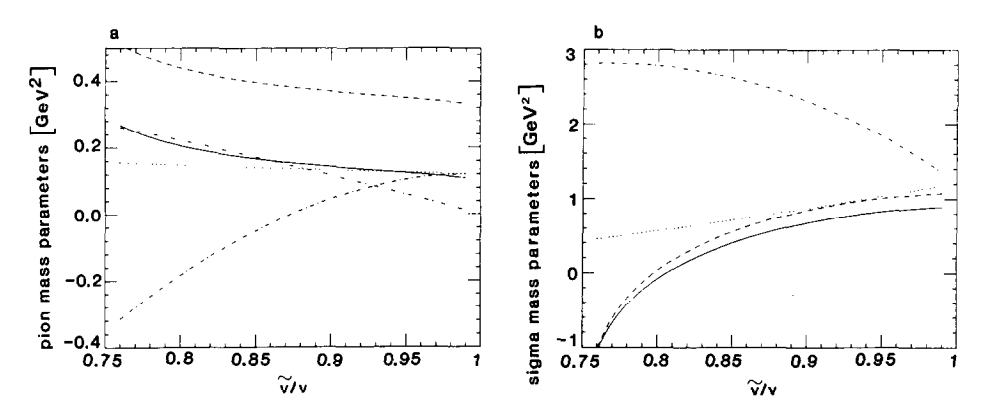


Fig. 8. Effective pion (a) and sigma (b) mass parameters for $\rho = 0.15$ fm⁻³ as functions of \tilde{v}/v . For explanation, see text.

the full lines in Fig. 9a coincide. Since $-\tilde{m}_{\pi}^2$ is an increasing function of the density (see Eq. (2.5c)), so is the self-energy $\Sigma_{\pi}(0)$. The square of the "pion effective mass"

$$M_{\pi}^{*2} = \tilde{m}_{\pi}^{2} + \Sigma_{\pi}(0) \tag{3.4}$$

is equal to $c/\tilde{v}_0 = m_\pi^2 \cdot v/\tilde{v}_0$ for every density. From Fig. 9b we see again that M_σ^{*2} is a decreasing function of the density. Actually it vanishes for $\rho \approx 0.16$ fm⁻³. A vanishing M_σ^{*2} means [4] that the Landau-Migdal parameter F_0 of the quasiparticle interaction approaches $-\infty$, and the system collapses due to the infinite amount of attraction.

Figures 8 and 9 also show the various contributions (3.3) to the self-energies. (The explicit expression of the mesonic contribution $\Sigma_{\alpha,\text{mes}}(0)$ is given in Appendix A.) The dotted lines in Figs. 8b, 9b show the quasiclassical mass parameter m_{α}^{*2} of Eq. (2.61a), the dashed-dotted line includes the Feynman part

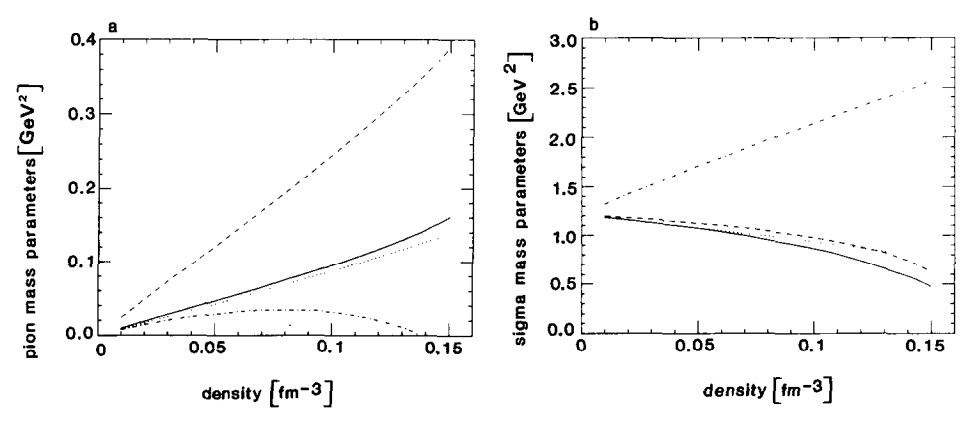


Fig. 9. Effective pion (a) and sigma (b) mass parameters as functions of the density. For explanation, see text.

 $\Sigma_{\sigma F}(0)$, and the dashed line includes further the mesonic piece $\Sigma_{\sigma, mes}(0)$. It is already well known [4] that in the quasiclassical approximation the σ mass is quenched, while the inclusion of the Feynman part $\Sigma_{\sigma F}$ gives rise to a very large enhancement. The former effect leads, as we discussed above, to a collapse of the system in the quasiclassical approximation, while the latter effect leads to a stabilization of the system once the one nucleon loop contribution to the energy density is added to the quasiclassical result. Figs. 8b, 9b, however, show that the meson loop term $\Sigma_{\sigma, mes}$ brings the σ mass again close to the quasiclassical result. We also see that the term $\delta \Sigma_{\sigma}$ of Eq. (3.3) due to the σNN vertex correction and the nucleon self-energy correction is small. In a similar way, the different contributions to the pion self-energy are shown in Figs. 8a, 9a. The dotted line shows the quasiclassical part $\Sigma_{\pi D}(0)$ and the dashed-dotted line also includes the Feynman part $\Sigma_{\pi F}(0)$. The latter one is negative and large. The meson loop term $\Sigma_{\pi, mes}$, however, gives a very large positive contribution, and the final result for $\Sigma_{\pi}(0)$ is again rather close to the quasiclassical part, $\Sigma_{\pi D}(0)$.

The above discussion on the meson self-energies shows the following two points: First, the reason for the instability of the system at normal densities ($\rho \gtrsim 0.16$ fm⁻³) is quite similar to the reason for the instability in the quasiclassical approximation: The effective σ mass (3.2b) is a decreasing function of the density and finally vanishes at normal densities, leading to an infinite amount of attraction in the Landau–Migdal force. Second, the very large positive contribution to the effective σ mass due to the Feynman part $\Sigma_{\sigma F}$, which in the one loop calculation [4] leads to a drastic weakening of the attraction and thereby to a stabilization of the system, is cancelled by the mesonic loop terms of Fig. 1b. A similar cancellation takes place also for the pion self-energy. This latter point, which will be taken up again in the next subsection, already gives us a hint that in the present model the nucleon and meson loops should be treated together.

Let us now discuss the individual contributions to the total binding energy per nucleon shown in Fig. 6a. A qualitative discussion of the various contributions has already been presented in Section 2.3. In the present approximation of neglecting the Feynman parts of the meson self-energies in the calculation of the energy density, we have $E_{(3)}^{\text{ex}} = E^{\text{V}} = 0$ in Eq. (2.49). The exchange energies $E_{(1)}^{\text{ex}}$ and $E_{(2)}^{\text{ex}}$ per nucleon are shown in Fig. 10. We see that the traditional exchange energy $E_{(1)}^{\rm ex}$ is small compared with the term $E_{(2)}^{\rm ex}$ due to $N\bar{N}$ excitations, and, moreover, the σ and ω contributions to $E_{(1)}^{\rm ex}$ tend to cancel each other. In the present calculation we do not use meson-nucleon vertex form factors. As we will see in the next subsection, $E_{(2)}^{\rm ex}$ is reduced very much if a vertex form factor is introduced. $E_{(2)}^{\rm ex}$ of Eq. (2.45c) is determined by the Feynman part of the nucleon self energy Σ_{NF} at $\tilde{k} = \tilde{m}_N$, which has been given in Eq. (2.52). For example, with the presently used parameters we have for $\rho = 0.13 \text{ fm}^{-3}$ $(\tilde{m}_N/m_N = 0.89)$, $\Sigma_{NF}(\tilde{k} = \tilde{m}_N) = (-52.0 + 224.2) \text{ MeV} =$ 172.2 MeV, where the first and second numbers are due to σ and ω , respectively. Altogether, we get a large repulsive contribution due to the exchange energies, which is mainly due to the ω meson term in $E_{(2)}^{\rm ex}$. The correlation energies $E^{\rm C}$ per nucleon are shown in Fig. 11. The dominant term is the large attractive longitudinal

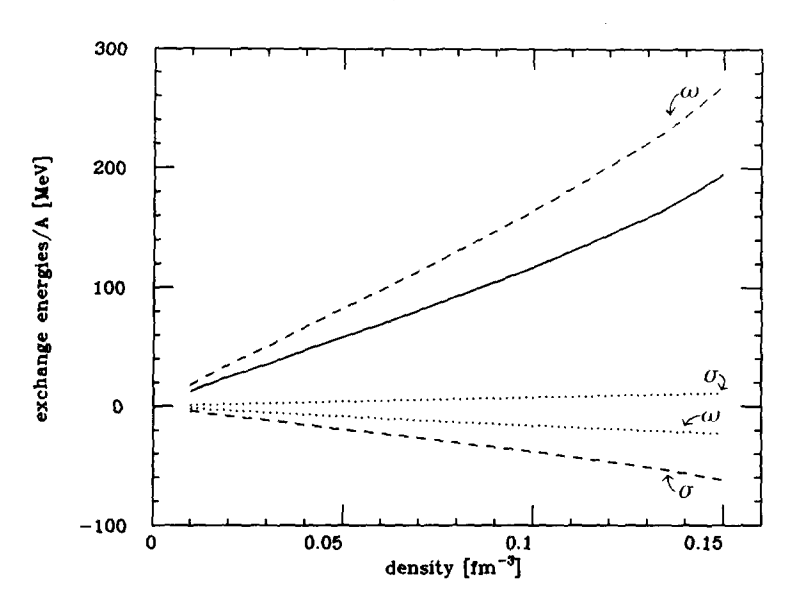


Fig. 10. The exchange energy contributions to the total binding energy per nucleon shown by the full line in Fig. 6a. Dotted lines, $E_{(1)}^{\rm ex}$; dashed lines, $E_{(2)}^{\rm ex}$; full line, total exchange energy contribution.

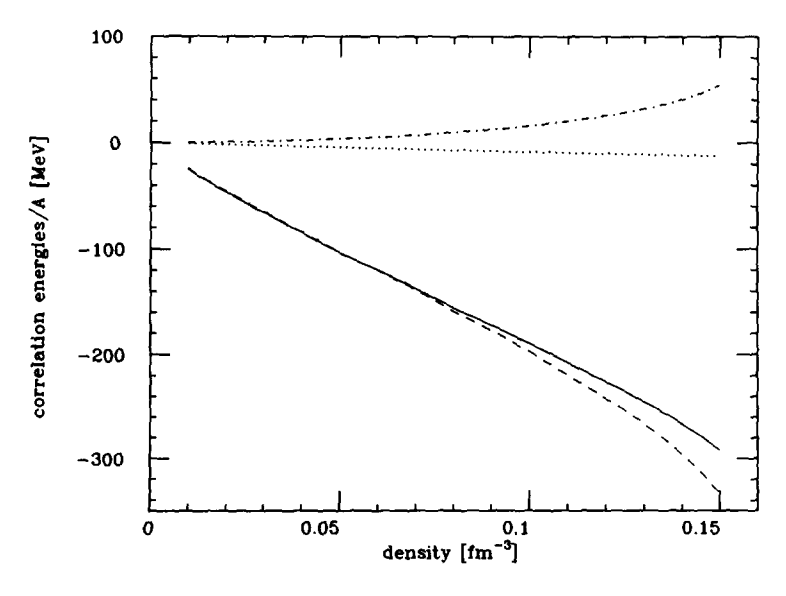


Fig. 11. The correlation energy contributions to the total binding energy per nucleon shown by the full line in Fig. 6a. Dashed-dotted line, $E_{\rm N}{}^C$; dotted line, $E_{\rm T}{}^C$; dashed line, $E_{\rm L}{}^C$; full line, total correlation energy contribution.

correlation energy E_L^C , which is partially cancelled by the nucleonic term E_N^C . In the Hartree approximation E_L^C reduces to (2.65). In a Hartree calculation employing high values of m_σ , as used also in the present calculation, this term is of the same order of magnitude as E_N^C with the opposite sign [3]. The additional large attraction shown in Fig. 11 comes mainly from the particle-hole excitations in the σ meson self-energy. Again we have to point out that the inclusion of vertex form factors would reduce E_L^C . The transverse contribution E_T^C is very small in spite of the large value for g_ω . Finally, the quasiclassical contribution (2.50) gives a large repulsion with the presently used high values for g_ω and m_σ . (For $\rho = 0.1$ fm⁻³ this term contributes about 60 MeV to E_B/A .) This fact, among others, probably points out the inadequacy of the present approximation: The lowest order term is highly repulsive, and all the attraction comes from the higher order correlations. Note that we were forced to use high values of g_ω and m_σ in order to satisfy condition (2.62b), or, more generally, (2.59a).

We mentioned above that for medium and high densities the conditions (2.62) are satisfied also for small values of \tilde{v}/v , suggesting the possibility of an abnormal state. Such a state, however, was not found in the actual calculation: If one uses large m_{σ} ($m_{\sigma} \gtrsim 1$ GeV), the condition (2.59a) turns out to be violated for finite $|\mathbf{k}|$. For smaller values of m_{σ} condition (2.59a) can be satisfied, but the energy per nucleon has a maximum at $\tilde{v} \approx 0$ rather than a minimum and, moreover, is positive and very large.

Alltogether, with the present approximation we are unable to give a satisfactory description of the nuclear matter binding energy: The saturation occurs at low densities and at medium and high densities nuclear matter is unstable. The reason for this instability is a pole in the two loop expression of the σ propagator at zero momentum. At low densities ($\rho \approx 0.1 \, \mathrm{fm}^{-3}$) the binding energy results from a delicate cancellation mainly between the attractive correlation energy and the repulsive exchange energy.

3.2. Feynman Parts of the Polarizations Included

We now wish to discuss how the situation changes when we include the Feynman parts of the polarizations (2.29) in the calculation of the energy density. It is clear from Eq. (2.61b) or Fig. (8b) that the piece $\Sigma_{\sigma F}(0)$ is very large and positive, at least for values of \tilde{v} relevant for the normal state. Its inclusion reduces the attractive contribution to the parameter $F_0^{(H)}$ of Eq. (2.61d) and thus makes condition (2.62b) easier to satisfy. This is reminiscent of the one loop (Hartree) calculation where the inclusion of the nucleon loop term in the energy density stabilizes the system. Due to the presence of this large positive piece in the σ propagator we can employ a small value for g_{ω} without violating (2.62b). For example, for the choice

$$m_{\omega} = 1.35 \text{ GeV}, \qquad g_{\omega} = 3.5$$
 (3.5)

Eq. (2.62b) leads to the restriction $0.55 \lesssim \tilde{v}/v \lesssim 0.95$ in the range of densities

0.1 fm⁻³ $\lesssim \rho \lesssim 0.4$ fm⁻³. (The upper limit imposed on the possible values of \tilde{v}/v is due to the fact that $\Sigma_{\sigma F}(0) \to 0$ as $\tilde{v} \to v$.)

In Section 2.3 we discussed the necessity to include meson-nucleon vertex form factors in order to prevent tachyon poles in the free space meson propagators. In the calculations to be discussed below we employ a dipole type form factor,

$$F(k^2) = \frac{-\Lambda^2}{k^2 - \Lambda^2},\tag{3.6}$$

choosing $\Lambda=850$ MeV. This means, in particular, that we multiply all meson self-energies by $F^2(k^2)$. Once this is done, the free space meson self-energies do not modify the propagators drastically. For example, with the parameters given above we have $|\hat{\Sigma}_{\sigma l}(l^2)/(l^2+m_{\sigma}^2)|<0.14$ for all l^2 . For the ω meson the influence of the free space self-energy is very small even for higher values of g_{ω} [11]. We will therefore approximate the meson propagators in free space by their lowest order forms. The form factors have also to be introduced into the nucleon self-energy (2.51a). This modifies the functions $f_{\alpha}^{(a)}(\mu^2, \mu^2)$ ($\mu = \tilde{m}_N$ or m_N) of Eq. (2.51b) as follows:

$$f_{\alpha}^{(a)}(\mu^{2}, \mu^{2}) \to f_{\alpha}^{(a)}(\mu^{2}, \mu^{2}; \Lambda^{2}) = \left(\frac{\Lambda^{2}}{\Lambda^{2} - m_{\alpha}^{2}}\right)^{2} \int_{0}^{1} dx \, x^{a} \ln \frac{\mu^{2}(1 - x)^{2} + m_{\alpha}^{2}x}{\mu^{2}(1 - x)^{2} + \Lambda^{2}x} + \frac{\Lambda^{4}}{\Lambda^{2} - m_{\alpha}^{2}} \int_{0}^{1} dx \, x^{a} \frac{x}{\mu^{2}(1 - x)^{2} + \Lambda^{2}x}.$$
 (3.7)

Introducing this modification into (2.52) we obtain the self-energy $\Sigma_{NF}(\tilde{p} = \tilde{m}_N)$ and $E_{(2)}^{ex}$ of Eq. (2.45c). The modified exchange energy $E_{(3)}^{ex}$ is obtained by multi-

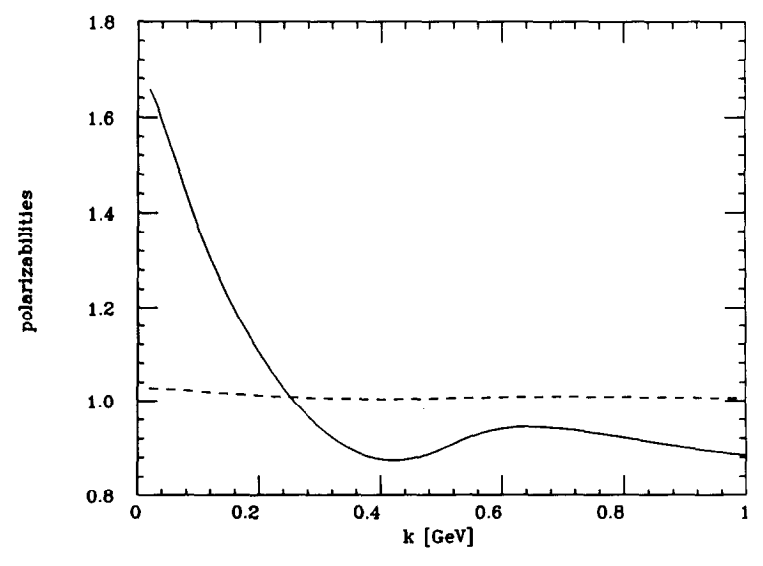


Fig. 12. Same as Fig. 5 for the case that the Feynman parts are included in the meson self-energies.

plying the polarizations in (2.55a) by $\hat{F}^2(l)$, introducing the replacement (3.7) into Eq. (2.55b) and leaving out the term (2.55c).

Figure 12 shows the longitudinal and transverse polarizabilities for the same case as in Fig. 5 ($\rho=0.15~{\rm fm}^{-3}$, $\tilde{v}/v=0.85$, and $\omega=20~{\rm MeV}$) using the parameters (3.5) and $\Lambda=850~{\rm MeV}$. For $|{\bf k}|\to 0$ the value of $\hat{\varepsilon}_{\rm L}$ is close to (2.60a). As we increase $|{\bf k}|$, the negative contribution of the particle-hole excitations in $\hat{\Pi}_{\sigma}$ of Eq. (2.64a) causes $\hat{\varepsilon}_{\rm L}$ to decrease. The mixing term $\hat{\Pi}_{\rm M}^2$ now plays a minor role due to the smaller g_{ω} . This is in contrast to the case shown in Fig. 5, where due to the large g_{ω} the particle-hole excitations in $\hat{\Pi}_{\rm M}^2$ dominate over those in $\hat{\Pi}_{\sigma}$, leading to a sharp increase for small $|{\bf k}|$.

In spite of the fact that the stability condition (2.59a) is now easier to satisfy, it turns out that we cannot improve the situation for the nuclear matter binding energy. On the contrary, even the saturation at low densities found in Section 3.1 is lost. The full line of Fig. 13a shows the binding energy per nucleon calculated with the parameters (3.5) and $\Lambda = 850$ MeV. The dotted line represents the quasiclassical contribution of Eq. (2.50). We found that, once the parameters are chosen such that one has binding at some medium densities (which in particular requires a high value for m_{σ} as we will discuss soon), at lower densities one has no binding, while at higher densities the binding energy increases until nuclear matter becomes unstable due to $M_{\sigma}^{*2} \to 0$ as found also in the previous subsection.

The binding energy per nucleon $E_{\rm B}/A$ of Fig. 13a shows a highly pathological behaviour. In particular, due to the general relations [4]

$$\rho \frac{d}{d\rho} (E_{\rm B}/A) = \delta \varepsilon_{\rm F} - E_{\rm B}/A \qquad (\delta \varepsilon_{\rm F} = \varepsilon_{\rm F} - m_{\rm N})$$
$$\frac{d\varepsilon_{\rm F}}{d\rho} = \frac{1}{N_{\rm F}} (1 + F_0)$$

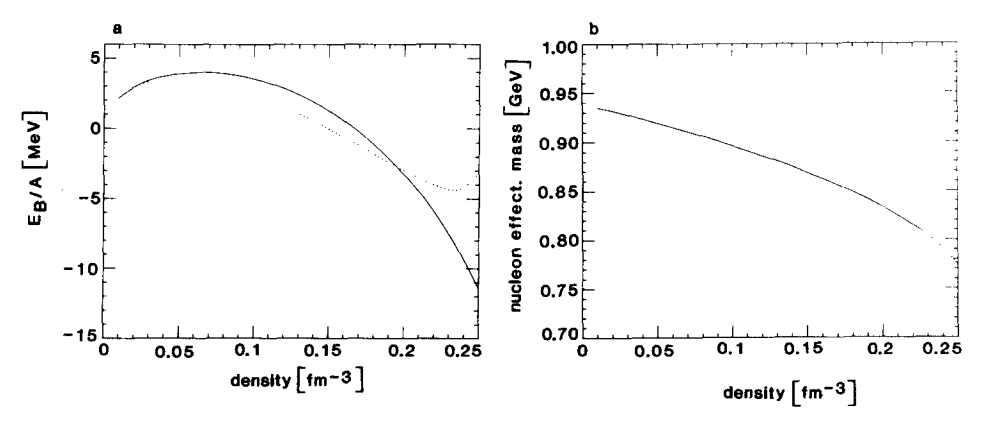


Fig. 13. Binding energy per nucleon (a) and the nucleon effective mass (b) calculated with the parameters (3.5) and A = 850 MeV. The Feynman parts of the meson self-energies are included. The dotted line in (a) shows the quasiclassical contribution and the full line the total result.

with ε_F the Fermi energy and N_F the density of states at the Fermi surface, it is seen that for small densities $\delta\varepsilon_F$ grows steeply, reaches a maximum before E_B/A of Fig. 13a reaches its maximum, and then falls off. The parameter F_0 decreases monotonously from positive to negative values. All these features are just opposite to those obtained from a saturating binding energy curve. Nevertheless, we will continue to discuss the results in detail, since some of the contributions to the binding energy will be left unmodified even if one goes beyond the present approximation scheme.

Selecting some densities, the binding energy per nucleon is plotted against \tilde{v}/v in Fig. 14. Again, as in Fig. 7, we find that beyond a certain density ($\rho \approx 0.26 \, \mathrm{fm}^{-3}$) the binding energy curves show no minima but decrease monotonously from their values at $\tilde{v}/v \approx 1$ until they enter the region $\tilde{v}/v < 0.55$, where Eq. (2.62b) is violated. According to our discussion in Section 3.1, this means that M_{σ}^{*2} of Eq. (3.2b) vanishes at $\tilde{v} = \tilde{v}_0$ for $\rho \approx 0.26 \, \mathrm{fm}^{-3}$. The π and σ mass parameters are shown in Figs. 15 and 16. Figure 15 illustrates Eqs. (3.2) for fixed $\rho = 0.2 \, \mathrm{fm}^{-3}$, and Fig. 16 shows the mass parameters as functions of the density. The curves in Figs. 15 and 16 are qualitatively very similar to those in Figs. 8 and 9, and therefore a similar discussion as given in Section 3.1 holds also here. Note that in this section we used the σ mass parameter $m_{\sigma}^{*2} + \Sigma_{\sigma F}(0)$, shown by the dashed-dotted lines in Figs. 15b and 16b, as an "input" in the calculation of the energy density, since our meson propagators now contain also the Feynman parts Σ_F besides the density parts Σ_D . Figures 15b and 16b, however, show that the "output" self-energy Σ_{σ} , which in addition contains also the meson loops and other two loop corrections, returns

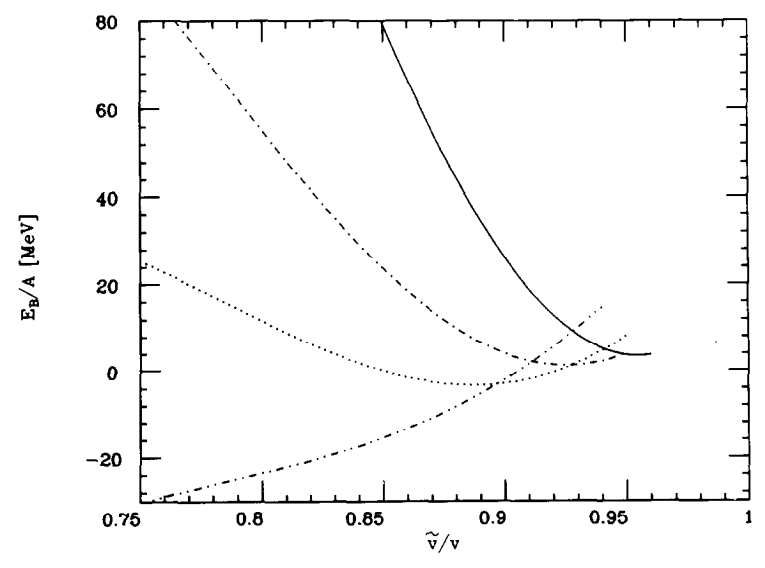


Fig. 14. Binding energy per nucleon as a function of \tilde{v}/v for various densities: 0.1 fm⁻³ (full line); 0.15 fm⁻³ (dashed-dotted line); 0.2 fm⁻³ (dotted line); 0.3 fm⁻³ (dashed double-dotted line). The case refers to the full line in Fig. 13a.

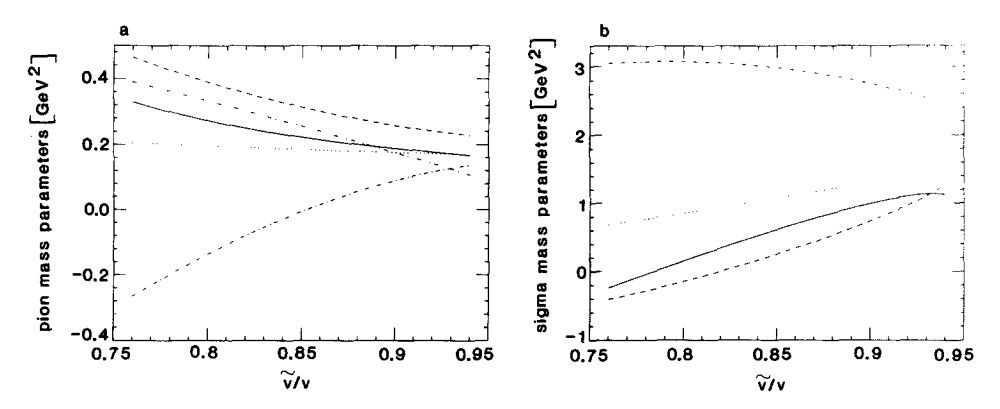


Fig. 15. Effective pion (a) and sigma (b) mass parameters for $\rho = 0.2$ fm⁻³ as functions of \tilde{v}/v . For explanation, see text.

towards the quasiclassical mass parameter m_{σ}^{*2} . The same feature is observed for the pion in Figs. 15a and 16a. This shows that, as far as the meson propagators are concerned, the present calculation is highly non-selfconsistent. We will come back to this point in the next subsection.

We now discuss the individual contributions to the binding energy per nucleon. Figure 17 shows the three parts of the exchange energy of Eq. (2.49). The contributions $E_{(1)}^{\rm ex}$ and $E_{(2)}^{\rm ex}$ can be compared with those in Fig. 10, noting that now we employ a much smaller g_{ω} and a meson-nucleon vertex form factor. From this comparison it is seen that the traditional exchange energies $E_{(1)}^{\rm ex}$ are not very sensitive to the cutoff, since the momentum transfer is limited, but the $E_{(2)}^{\rm ex}$ are very sensitive. Namely, the use of $\Lambda=850$ MeV reduces them by a factor 8 to 9 compared to the case $\Lambda=\infty$. The new contribution $E_{(3)}^{\rm ex}$ has already been discussed qualitatively in Section 2.3, and we have the following contributions to Eq. (2.55) for $\rho=0.2$ fm⁻³ ($\tilde{m}_{\rm N}/m_{\rm N}=0.89$): The unrenormalized free space nucleon self-

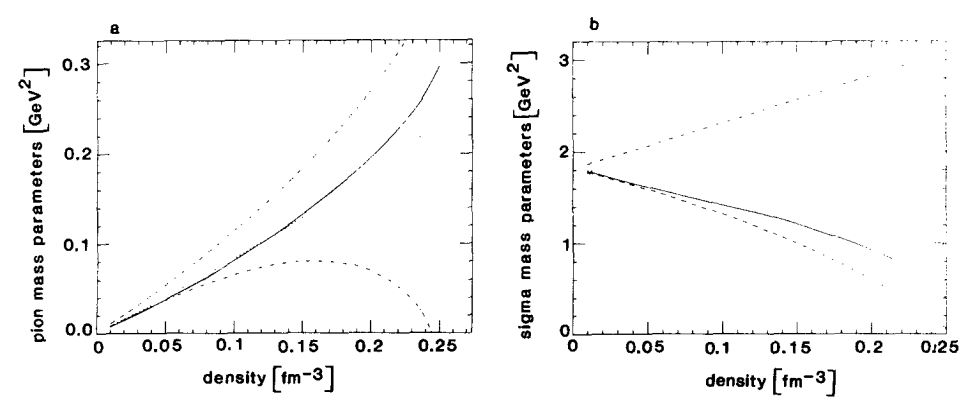


Fig. 16. Effective pion (a) and sigma (b) mass parameters as functions of the density. For explanation, see text.

energy (i.e., the term [...] in Eq. (2.55b)) takes the value $\bar{\Sigma}_{NF}(k=m_N)$ (-127.4 + 44.8) MeV = -82.6 MeV, where the first and second numbers are due to σ and ω , respectively. The constant C takes the value $C = -0.00246 \,\text{GeV}^4$. As discussed before, the sign of $E_{(3)}^{ex}$ is determined by the term (2.55b), which dominates over (2.55a). As in all parts of the exchange energy, σ and ω tend to cancel each other. Figure 18 shows the contribution due to the fourth order term (2.56). Since the ω contribution is negligiblely small, we show only the term due to the σ meson. As discussed in Section 2.3, it depends very sensitively on m_{σ} and, moreover, also on the cutoff mass Λ . For high values of m_a we have attraction as shown in Fig. 18. Although E^{V} is finite for $\Lambda \to \infty$, it becomes unphysically large in this limit. The correlation energies are shown in Fig. 19. Again we encounter a very high sensitivity to m_{σ} : The longitudinal correlation energy $E_{\rm L}^{\ C}$ gives attraction only for high values of m_{α} . The possibility to have a repulsive longitudinal correlation energy is due to the large positive Feynman part $\Sigma_{\sigma F}$. As m_{σ} increases, the (negative) mass shift δ_{σ} becomes increasingly important and the whole contribution turns into an attractive one. This feature, together with the behaviour of E^{V} discussed before, forces one to use high m_{σ} in order to have attraction at least for some densities.

In our calculation including the Feynman part of the σ self-energy, the abnormal state is pratically ruled out by the condition (2.60a). This is so since at $\tilde{v} \approx 0$ the piece $\Sigma_{\sigma F}(0)$ is negative and very large in magnitude. Only at extremely high densities the term m_{σ}^{*2} in (2.60a) dominates over $\Sigma_{\sigma F}(0)$, see Ref. [4].

In conclusion of this part, the use of the full nucleon loop term in the meson selfenergies does not improve the situation for the nuclear matter binding energy found

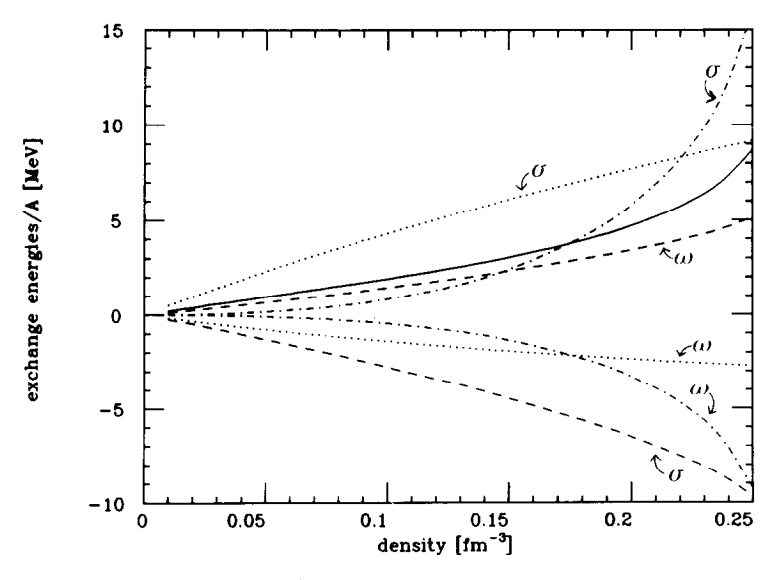


Fig. 17. The exchange energy contributions to the total binding energy per nucleon shown by the full line in Fig. 13a. Dotted lines, $E_{(1)}^{\text{ex}}$; dashed lines, $E_{(2)}^{\text{ex}}$; dashed-dotted lines, $E_{(3)}^{\text{ex}}$; full line, total exchange energy contribution.

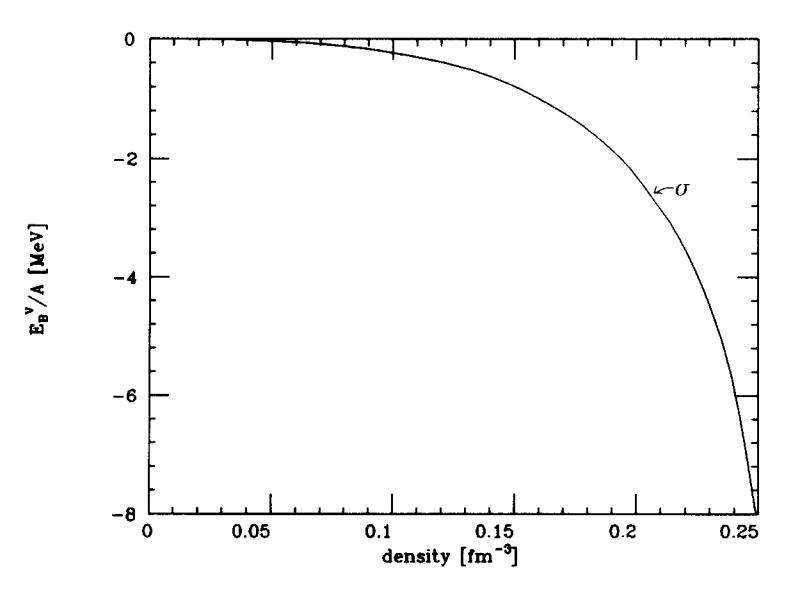


Fig. 18. The contribution of the σ meson term in E^{V} of Eq. (2.56) to the total binding energy per nucleon shown by the full line in Fig. 13a.

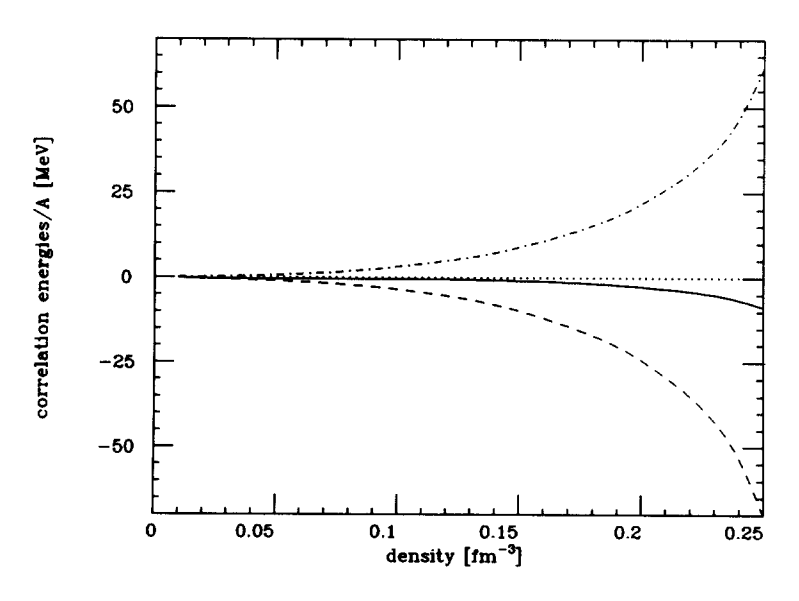


Fig. 19. The correlation energy contributions to the total binding energy per nucleon shown by the full line in Fig. 13a. Dashed-dotted line, E_N^C ; dotted line, E_L^C ; dashed line, E_L^C ; full line, total correlation energy contribution.

in Section 3.1, but on the contrary makes it worse: There is no saturation as a function of the density, and beyond some density ($\rho \approx 0.26 \, \mathrm{fm^{-3}}$ in the present calculation), the system becomes unstable with respect to variations in \tilde{v} . The reason for this instability is the same as found in the previous subsection; i.e., as we approach this density from below, the σ meson exchange part of the Landau–Migdal force gives an infinite amount of attraction.

3.3. Role of the Meson Loops in the Meson Polarizations

In the last two subsections we have seen that the two approximations introduced in Section 2.2 (see the discussion around Eq. (2.18)) are not appropriate for a description of the nuclear matter binding energy. If we avoid the approximation (2.18), our developments have to be changed in the following respects: First, we have to take into account the two line irreducible meson loop contributions in Eq. (2.17), and second, due to the variational principle, the meson self-energies also include the meson loop diagrams shown in Fig. 1. We have to say little about the former effect, but we wish to discuss some points concerning the latter one. Actually, we have already seen in Figs. 8, 9, 15, and 16 that these meson loops affect the total meson self-energies very much. For k = 0, the large nucleon loop contribution due to Σ_{aF} is cancelled by the meson loops. In the Hartree approximation, the cancellation between the diagrams of Figs. 1a and b can be understood as follows: In this approximation, the correlation energies are given by (2.58) and (2.65). The nucleonic contribution (2.58) is due to the negative energy Dirac sea, while the mesonic contribution (2.65) comes from the positive energy bosonic zero-point oscillations. The cancellation between these two terms is physically quite transparent and has been discussed in many previous works [1, 3, 4]. The first and second derivatives of these terms with respect to $x = \tilde{v}/v$ determine the pion selfenergies of Figs. 2a and b, and the σ self-energies of Figs. 1a and b, respectively. Since the dependence of (2.58) and (2.65) on x is similar ((2.58) is a function of $x^2 = 1 + (x^2 - 1)$ and (2.64) is the same function of $1 + \frac{3}{2}(x^2 - 1)$, it follows that there is also a cancellation between the nucleon loop and meson loop diagrams of Figs. 1 and 2. This observation further supports our supposition that in our model the fermionic and bosonic terms should be taken into account simultaneously.

An exact assessment of the meson loops goes beyond the scope of the present work. In principle, as mentioned above, we should solve the Dyson equation which now appears as an integral equation, then use the modified σ self-energy in the calculation of the correlation energy (2.63), and include also additional mesonic two loop diagrams in the energy density. In this section we only wish to estimate the influence of the additional meson self-energies on the longitudinal correlation energy (2.63a). The forms of the mesonic pieces $\Sigma_{\alpha, \text{mes}}$ ($\alpha = \sigma, \pi$) have been given in Appendix A. In the Hartree approximation they reduce to [4]

$$\Sigma_{\pi, \text{mes}}(0) = \frac{3\lambda^2 m_{\sigma}^2}{16\pi^2} G(y_{\sigma})$$
 (3.8a)

with

$$G(y_{\sigma}) = y_{\sigma} \ln y_{\sigma} - y_{\sigma} + 1; \qquad y_{\sigma} = \frac{\tilde{m}_{\sigma}^{2}}{m_{\sigma}^{2}};$$
 (3.8b)

and

$$\Sigma_{\sigma,\text{mes}}(0) = \frac{\partial}{\partial \tilde{v}} \left(\tilde{v} \Sigma_{\pi,\text{mes}}(0) \right)$$
 (3.8c)

$$=\frac{3\lambda^2 m_\sigma^2}{16\pi^2}H(y_\sigma) \tag{3.8d}$$

with

$$H(y_{\sigma}) = \left(y_{\sigma} + \tilde{v}\frac{\partial y_{\sigma}}{\partial \tilde{v}}\right) \ln y_{\sigma} - y_{\sigma} + 1.$$
 (3.8e)

To avoid the tachyon pole we replace $y_{\sigma} \to y_{\sigma}^* = m_{\sigma}^{*2}/m_{\sigma}^2$ with the quasiclassical σ mass parameter of Eq. (2.61a). As in other cases [4], this ad hoc replacement is not unique. One can perform this substitution in (3.8a) and then calculate $\Sigma_{\sigma,\text{mes}}(0)$ from the general relation (3.8c) between the π and σ self-energies at k=0. In this case, which we will call prescription (a), one has $y_{\sigma} \to y_{\sigma}^*$ in (3.8d), (3.8e). Likewise, one could first calculate $\Sigma_{\sigma,\text{mes}}(0)$ in the pure Hartree approximation and then substitute $y_{\sigma} \to y_{\sigma}^*$ (prescription (b)). The results differ due to the derivative term in (3.8e). We will show the results obtained with both prescriptions.

The piece (3.8d) is negative for $y_{\sigma} < 1$ (or $y_{\sigma}^* < 1$) and cancels large parts of the nucleon loop term $\Sigma_{\sigma F}(0)$. In order to estimate the effect of this cancellation on the binding energy, we simply add (3.8d) to the σ polarization \hat{H}_{σ} in the expression for the longitudinal correlation energy (2.63a), leaving the other parts of the energy density unchanged. This is, off course, a very crude and, moreover, non-unique treatment. Nevertheless, it might provide insight into the way an additional self-energy piece which strongly cancels with the large $\Sigma_{\sigma F}$ affects the results for the binding energy.

It turns out that the above prescriptions lead to a saturating nuclear matter state. We found that one can choose many possible parameter sets $(g_{\omega}, m_{\sigma}, \Lambda)$ with similar results. Here we use the set

$$g_{co} = 5.5, \qquad m_{\sigma} = 0.84 \text{ GeV}, \qquad \Lambda = 0.835 \text{ GeV}.$$
 (3.9)

Figure 20 shows the results for the binding energy per nucleon and the effective nucleon mass. We plot the quasiclassical contribution and the total binding energy per nucleon obtained with both prescriptions (a) and (b). With the parameter set (3.9), the condition (2.62b) cannot be satisfied for densities $\rho \leq 0.04$ fm⁻³; i.e., nuclear matter is unstable at very small densities. For any reasonable parameter set one finds that prescription (a) tends to give too low saturation densities ($\rho \approx 0.13$ fm⁻³). From Fig. 20a it is seen that the total loop correction to be

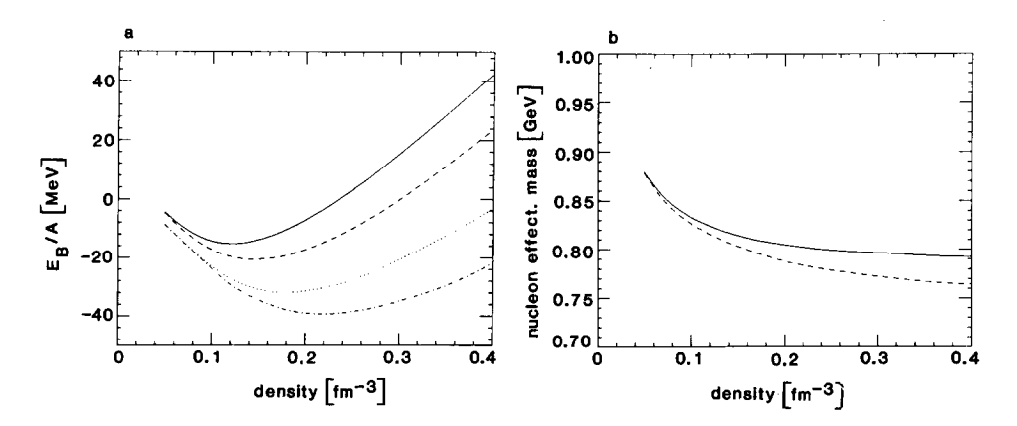


Fig. 20. Binding energy per nucleon (a) and the nucleon effective mass (b) calculated with the parameters (3.9). The Feynman parts of the meson self-energies are included, and the meson loops are incorporated as described in the text. In Fig. (a), the results obtained with prescription (a) are shown by the dotted line (quasiclassical contribution) and the full line (total result), while prescription (b) gives the dashed-dotted line (quasiclassical contribution) and the dashed line (total result). The full (dashed) line in Fig. (b) refers to prescription (a) ((b)).

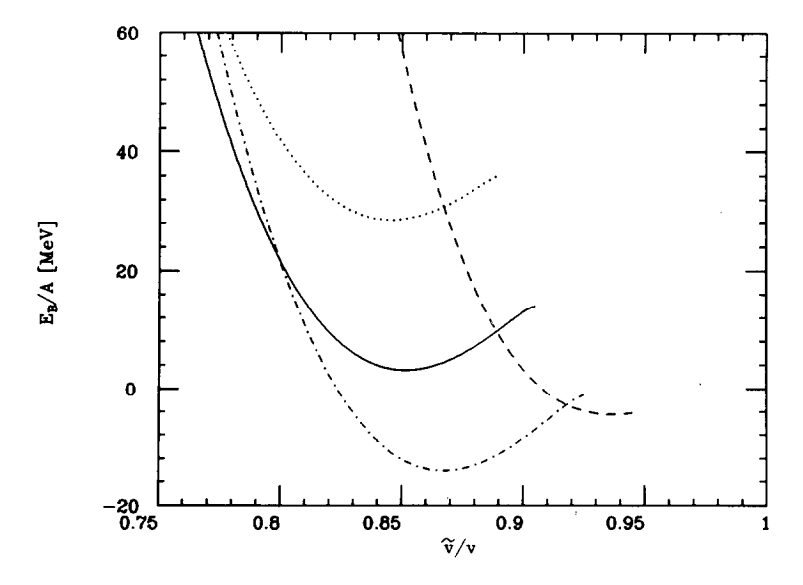


Fig. 21. Binding energy per nucleon as a function of \tilde{v}/v for various densities: 0.05 fm⁻³ (dashed line); 0.15 fm⁻³ (dashed-dotted line); 0.25 fm⁻³ (full line); 0.35 fm⁻³ (dotted line). The case refers to the full line in Fig. 20a.

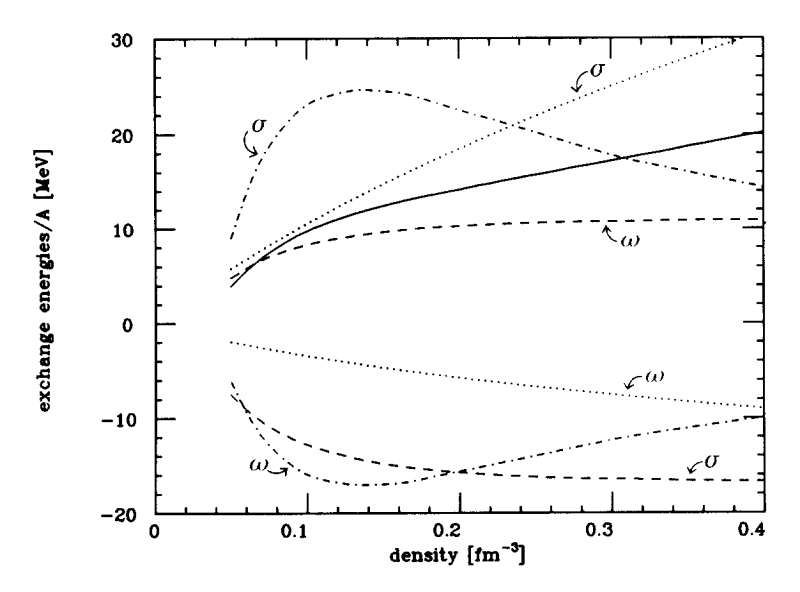


Fig. 22. The exchange energy contributions to the total binding energy per nucleon shown by the full line in Fig. 20a. Dotted lines, $E_{(1)}^{\rm ex}$; dashed-lines, $E_{(2)}^{\rm ex}$; dashed-dotted lines, $E_{(3)}^{\rm ex}$; full line, total exchange energy contribution.

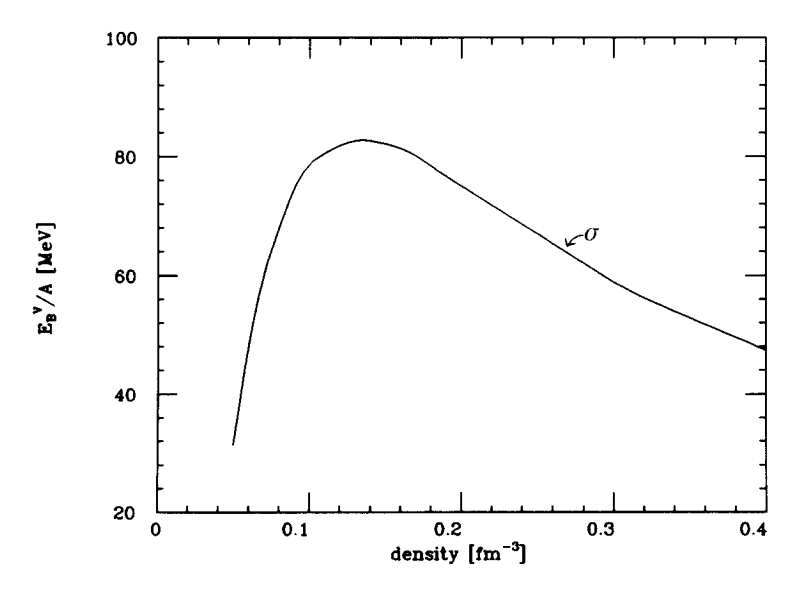


Fig. 23. The contribution of the σ meson term in E^{V} of Eq. (2.56) to the total binding energy per nucleon shown by the full line in Fig. 20a.

discussed below is repulsive. The results shown in the following refer to prescription (a).

Figure 21 shows the binding energy for some fixed densities as a function of \tilde{v}/v and should be compared with the previous results in Figs. 7 and 14. Since the present treatment is only an approximate one, we will not repeat the entire discussions on the effective meson mass parameters here. We just note that M_{σ}^{*2} of Eq. (3.2b) is now an increasing function of the density, as can also be seen from the curves in Fig. 21.

The individual contributions to the binding energy are shown in Figs. 22 to 24. Consider first the correlation energies of Fig. 24. Since the large positive piece $\Sigma_{\sigma F}$ is largely cancelled in the present calculation, the longitudinal correlation energy E_L^C is again strongly attractive as in Section 3.1. In particular, we are not forced anymore to employ high values for m_{σ} in order to get attraction from the correlation energy. The exchange energies of Fig. 22 show a behaviour which is qualitatively similar to Fig. 17, except for the larger $E_{(3)}^{ex}$. As in all previous cases, the total exchange energy is repulsive. The contribution of the fourth-order term E^V is shown in Fig. 23. For the presently adopted lower value of m_{σ} the second term in the numerator of (2.56) dominates the first term, leading to a strongly repulsive contribution.

The above findings are summarized as follows: If the meson loop contribution to the σ self-energy, Eq. (3.8d), is invoked in order to cancel the large nucleon loop term $\Sigma_{\sigma F}$ in the correlation energy, we are able to account for the saturation properties of nuclear matter. The quasiclassical contribution itself is saturating, and

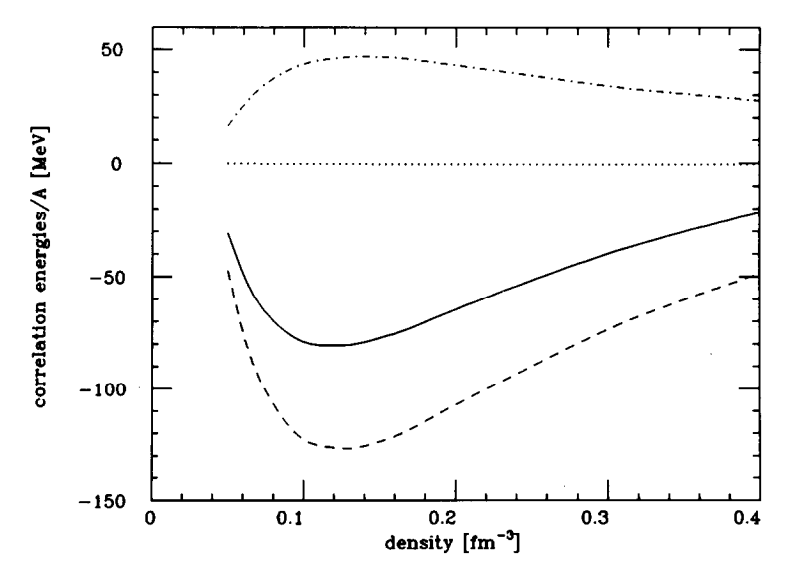


Fig. 24. The correlation energy contributions to the total binding energy per nucleon shown by the full line in Fig. 20a. Dashed-dotted line, E_N^C ; dotted line, E_L^C ; dashed line, E_L^C ; full line, total correlation energy contribution.

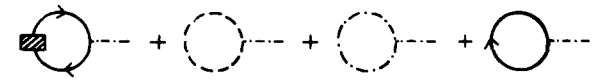


Fig. 25. Graphical representation of Eq. (A.4). For explanation of the symbols, see the caption to Fig. 1.

the total loop correction to it is repulsive, resulting from a cancellation between the attractive correlation energy and the repulsive fourth-order term E^{V} and the exchange energies.

4. SUMMARY AND CONCLUSIONS

In this paper we studied the binding energy of nuclear matter in the chiral σ - ω model. Our motivation for choosing this model was to incorporate some of the general chiral symmetry constraints [4, 5] into an actual nuclear matter calculation. For the calculation of the binding energy we used an approximation to the Hartree-Fock scheme. This approximation consisted in the following: First, we neglected the two-line irreducible meson loops and, second, we used the nucleon Hartree propagator S_0 is order to construct the meson self-energies. Our finding is that these approximations do not allow an adequate description of nuclear matter. We arrived at this conclusion in two steps: In the first one we took into account only the explicitly density dependent part of the meson self-energies, leaving out the vacuum polarization pieces. We then found: (a) The stability condition (2.59a) is too stringent due to the large attraction from the σ meson exchange potential. We pointed out that for the same reason nuclear matter is unstable in the quasiclassical approximation. One must use rather high values for m_{σ} and g_{ω} , which leads to a very repulsive quasiclassical contribution to the binding energy. Moreover, the possible range of values for \tilde{v}/v is very limited, and this restriction is not relaxed very much as the density increases, except for very high densities. (b) Nuclear matter is unstable for densities $\rho \gtrsim 0.16$ fm⁻³. The reason for this is that the effective σ mass parameter (3.2b) including the two loop contributions is a decreasing function of the density and vanishes around $\rho \approx 0.16$ fm⁻³. It is, however, possible to achieve saturation of the binding energy for smaller densities.

In the second step we included the vacuum polarization pieces in the meson propagators. This actually means to add a very large positive term to the σ meson self-energy. We found: (a) The stability conditions are then less stringent. (For the same reason nuclear matter is stable in the Hartree approximation if one adds the nucleon loop contribution to the quasiclassical result.) Nevertheless, (b) the binding energy does not saturate, and for $\rho \gtrsim 0.26$ fm⁻³ nuclear matter is unstable. The reason for this instability is similar to the one discussed before: Though we now use a highly enhanced effective σ mass (i.e., $m_{\sigma}^{*2} + \Sigma_{\sigma F}(0)$) in the calculation of the energy density, the final σ mass parameter (3.2b) decreases with increasing density and vanishes for $\rho \approx 0.26$ fm⁻³. Contrary to the case discussed before, it is not possible to achieve saturation before this density is reached. Rather, the attraction increases without limits as we approach this density from below.

One by-product of the above calculation was the finding that the cancellation of the large vacuum polarization contribution to M_{σ}^{*2} comes mainly from the meson loops in the σ self-energy. We pointed out that in the Hartree approximation this cancellation is physically quite transparent, since it can be traced back to the cancellation between negative energy fermionic and positive energy bosonic zero point oscillation energies. We included the effect of the meson loops in a very rough manner in the correlation energy, neglecting all additional modifications. We found that this leads to a saturating nuclear matter state without instabilities even at high densities. The quasiclassical contribution itself saturates, and the loop contributions give an overall repulsion.

Here let us make a few remarks concerning the pionic contributions, which we did not consider in the present work. If the pion is included in the two steps discussed above, one meets the following difficulties: In the first step (vacuum polarizations neglected) pion condensation occurs and makes the pionic correlation energy complex. The attractive particle-hole contributions cause the pionic polarizability to become negative for $\omega \approx 0$ and finite |k|. What remains from the large cancellation between the repulsive $N\bar{N}$ Pauli correction piece and the attractive contribution due to the $\sigma\pi^2$ coupling is a repulsive contribution to the pion self-energy, but this is not sufficient to prevent pion condensation. This instability, which is similar to the one discussed for the transverse ω meson contribution in Section 2.3, can be avoided by including a phenomenological two-body force which in the nonrelativistic limit reduces to the familiar $g'(\sigma_1 \cdot \sigma_2)(\tau_1 \cdot \tau_2)$ -type interaction [15]. More serious difficulties come up in the second step: As is clear from Figs. 8a and 9a, the vacuum polarization contribution to the pion self-energy is negative and very large. As a result, even for small deviations of \tilde{v}/v from unity, the pionic mode becomes unstable. However, as we discussed in Section 3, there are again large cancellations due to the meson loop contributions to the pion self-energy. Thus, if the pion is included, the consideration of the meson loop contributions becomes ever more important.

Our above discussion indicates that in the chiral σ - ω model one should always take into account the fermionic and bosonic contributions on the same footing. This was pointed out earlier for the case of the Hartree approximation [1, 3] and persists if the exchange and correlation energies are included. A quantitative assessment of the bosonic loop contributions is a challenging task for future works.

APPENDIX A

(1) Demonstration of the Relations (2.23) in the Present Approximation

First we differentiate the energy density (2.22) with respect to \tilde{v} . We have, from Eqs. (2.13), (2.14), (2.9c), and (2.8b),

$$\frac{\partial}{\partial \tilde{v}} (U + \delta U) = \tilde{v} (\tilde{m}_{\pi}^{2} + \delta \tilde{m}_{\pi}^{2}) - c. \tag{A.1}$$

For the derivative of the loop part E_L we have

$$S_{\sigma} = -i \frac{\partial E_{L}}{\partial \tilde{v}}$$

$$= -\int \frac{d^{4}k}{(2\pi)^{4}} \left\{ \operatorname{Tr} \left[\left(S_{0}^{-1} \frac{\partial S_{0}}{\partial \tilde{v}} \right) + g(Z_{g} - 1) S_{0} + g S_{0}^{2} (\delta \tilde{m}_{N} - \tilde{k}(Z_{N} - 1)) \right] \right\}$$

$$+ \frac{1}{2} \int \frac{d^{4}k}{(2\pi)^{4}} \left\{ \operatorname{Tr} \left(\Delta^{-1} \frac{\partial \Delta}{\partial \tilde{v}} \right) + 3 \Delta_{\pi}^{-1} \frac{\partial \Delta_{\pi}}{\partial \tilde{v}} \right\}. \tag{A.2}$$

Here we used (2.8a). Performing a partial integration in the last two terms we get, using (2.20b), (2.20c) and the forms (2.16),

$$S_{\sigma} = -\int \frac{d^{4}k}{(2\pi)^{4}} \left\{ gZ_{g} \operatorname{Tr} S_{0} + g \operatorname{Tr} \left[S_{0}^{2} (\delta \tilde{m}_{N} - \tilde{k}(Z_{N} - 1)) \right] \right\}$$

$$+ 3\lambda^{2} Z_{\lambda} \tilde{v} \int \frac{d^{4}k}{(2\pi)^{4}} (\Delta_{\sigma} + \Delta_{\pi}) + \frac{1}{2} \int \frac{d^{4}k}{(2\pi)^{4}} \left\{ \operatorname{Tr} \Delta \frac{\partial \bar{\Sigma}}{\partial \tilde{v}} + 3\Delta_{\pi} \frac{\partial \bar{\Sigma}_{\pi}}{\partial \tilde{v}} \right\}.$$
 (A.3)

Using the forms of the unrenormalized self-energies (see Eqs. (2.29) for $\bar{\Sigma}$), we arrive at

$$S_{\sigma} = -gZ_{g} \int \frac{d^{4}k}{(2\pi)^{4}} \operatorname{Tr} S_{0} + 3\lambda^{2} Z_{\lambda} \tilde{v} \int \frac{d^{4}k}{(2\pi)^{4}} (\Delta_{\sigma} + \Delta_{\pi})$$
$$-g \int \frac{d^{4}k}{(2\pi)^{4}} \operatorname{Tr} (S_{0}^{2} \Sigma_{N}). \tag{A.4}$$

Here the quantity Σ_N is the one loop nucleon self-energy constructed from the full meson propagators Δ and Δ_{π} . S_{σ} is shown graphically in Fig. 25. We now show the relation

$$\frac{i}{\tilde{v}}S_{\sigma} = \bar{\Sigma}_{\pi}(0) = A_{\pi} + B_{\pi} \tag{A.5}$$

with the nucleonic contribution (see Figs. 2a, c)

$$A_{\pi} = ig^{2} \int \frac{d^{4}k}{(2\pi)^{4}} \operatorname{Tr} \left\{ Z_{g} \gamma_{5} S_{0} \gamma_{5} S_{0} + \gamma_{5} S_{0} \frac{\Lambda_{\pi}(k, k)}{g} S_{0} + 2\gamma_{5} S_{0} \gamma_{5} S_{0} \Sigma_{N} S_{0} \right\}$$
(A.6)

and the mesonic contribution (see Fig. 2b)

$$B_{\pi} = i\lambda^2 Z_{\lambda} \int \frac{d^4k}{(2\pi)^4} (\Delta_{\sigma} + 5\Delta_{\pi} + 2i\tilde{v}\Delta_{\sigma}\Delta_{\pi}T(-k;k,0)). \tag{A.7}$$

Concerning the mesonic vertices T, we follow the notations and conventions of Lee, Ref. [5]. The πNN vertex correction Λ_{π} in (A.6) satisfies [4]

$$\Lambda_{\pi}(k,k) = \frac{1}{2\tilde{v}} \left\{ \gamma_5, \Sigma_{N} \right\}. \tag{A.8}$$

Putting this relation into (A.6), one finds

$$A_{\pi} = -i \frac{g^2}{\tilde{m}_{\rm N}} Z_g \int \frac{d^4k}{(2\pi)^4} \operatorname{Tr} S_0 - i \frac{g^2}{\tilde{m}_{\rm N}} \int \frac{d^4k}{(2\pi)^4} \operatorname{Tr} (S_0^2 \Sigma_{\rm N}). \tag{A.9}$$

The $\sigma\pi^2$ vertex in (A.7) satisfies [4, 5]

$$\tilde{v}T(-k; k, 0) = i(\Delta_{\sigma}^{-1} - \Delta_{\pi}^{-1}),$$
 (A.10)

and using this we obtain

$$B_{\pi} = 3i^2 Z_{\lambda} \int \frac{d^4k}{(2\pi)^4} (\Delta_{\sigma} + \Delta_{\pi}). \tag{A.11}$$

From Eqs. (A.4), (A.9), and (A.11) we see that Eq. (A.5) is satisfied.

Let us now turn to the second derivative of the energy density will respect to \tilde{v} . We have

$$\frac{\partial^2}{\partial \tilde{v}^2} (U + \delta U) = \tilde{m}_{\sigma}^2 + \delta \tilde{m}_{\sigma}^2, \tag{A.12}$$

as follows from (A.1), (2.5), and (2.9). In order to calculate the derivative of (A.4), we use the relations

$$\Lambda_{\sigma}(k, k) = -i \frac{\partial \Sigma_{N}(k)}{\partial \tilde{v}} \qquad (\sigma NN \text{ vertex correction})$$

$$T(0; k, -k) = i \frac{\partial \Lambda_{\pi}^{-1}(k)}{\partial \tilde{v}} \qquad (\sigma \pi^{2} \text{ vertex})$$

$$T(0, k, -k;) = i \frac{\partial \Lambda_{\sigma}^{-1}(k)}{\partial \tilde{v}} \qquad (\sigma^{3} \text{ vertex}).$$
(A.13)

Then we obtain

$$\frac{\partial^2 E_{\rm L}}{\partial \tilde{v}^2} = i \frac{\partial S_{\sigma}}{\partial \tilde{v}} = \bar{\Sigma}_{\sigma}(0) = A_{\sigma} + B_{\sigma} \tag{A.14}$$

with the nucleon loop contribution (see Figs. 1a, c)

$$A_{\sigma} = \frac{\partial}{\partial \tilde{v}} (\tilde{v} A_{\pi}) = -ig^2 \int \frac{d^4k}{(2\pi)^4} \operatorname{Tr} \left\{ Z_g S_0^2 + iS_0^2 \frac{\Lambda_{\sigma}(k, k)}{g} + 2S_0^3 \Sigma_N \right\}$$
 (A.15)

and the meson loop contribution (see Fig. 1b)

$$B_{\sigma} = \frac{\partial}{\partial \tilde{v}} (\tilde{v} B_{\pi}) = 3i\lambda^{2} Z_{\lambda} \int \frac{d^{4}k}{(2\pi)^{4}} (\Delta_{\sigma} + \Delta_{\pi})$$
$$-3\lambda^{2} \tilde{v} Z_{\lambda} \int \frac{d^{4}k}{(2\pi)^{4}} (\Delta_{\sigma} T(0, k, -k;) \Delta_{\sigma} + \Delta_{\pi} T(0; k, -k) \Delta_{\pi}). \tag{A.16}$$

Equations (A.5) and (A.14) are the expressions for the unrenormalized π , σ self-energies which are consistent with our expression (2.22) for the energy density. In the actual calculation described in the main text we leave out the pionic term in E_L of Eq. (2.22b). In this case the quantity S_{σ} (see Eq. (A.4)) does not include the term involving Δ_{π} . Consequently, also in the quantities B_{π} (Eq. (A.11)) and B_{σ} (Eq. (A.16)) we have to leave out the terms involving Δ_{π} .

(2) Formulae for the Meson Loop Terms

Our applications in Sect. 3 require the forms of the meson loop contributions (A.11) and (A.16) for the case that Δ_{σ} is constructed from the nucleon loop term including the σ - ω mixing and that the term involving Δ_{π} is neglected. Δ_{σ} can be expressed conveniently by using the longitudinal polarizability ε_{L} of (2.33a) as follows:

$$\Delta_{\sigma}^{-1}(k) = k^2 - m_{\sigma}^2 - \Pi_{\sigma} + \frac{\Pi_{M}^2}{k^2 - m_{\sigma}^2 + \Pi_{M}}$$
 (A.17a)

$$= \varepsilon_{\rm L} \frac{\Delta_{\rm of}^{-1}}{1 - \Delta_{\rm of} \Pi_{\rm L}}.$$
 (A.17b)

The last term in (A.17a) is the σ self-energy with intermediate one ω meson states; i.e., the effect of the σ - ω mixing. Relation (A.17b) is easily derived from (A.17a) by using the form (2.33a). Therefore the σ meson part of (A.11) is given by ($Z_{\lambda} = 1$ in the present approximation)

$$\bar{\Sigma}_{\pi,\text{mes}}(0) = 3i\lambda^2 \int \frac{d^4k}{(2\pi)^4} \Delta_{\sigma}(k)$$

$$= 3i\lambda^2 \int \frac{d^4k}{(2\pi)^4} (\Delta_{\sigma} - \Delta_{\sigma f} - (\Pi_{\sigma F} + \delta_{\sigma}) \Delta_{\sigma f}^2) \tag{A.18a}$$

$$+3i\lambda^2 \int \frac{d^4k}{(2\pi)^4} \left(\Delta_{\sigma f} + (\Pi_{\sigma F} + \delta_{\sigma}) \Delta_{\sigma f}^2\right). \tag{A.18b}$$

The term (A.18a) is finite as follows from (2.54a) and from $\Pi_{\sigma D} \propto 1/k^2$ for $k \to \infty$. The renormalized self-energy is then given by

$$\Sigma_{\pi, \text{mes}}(0) = \overline{\Sigma}_{\pi, \text{mes}}(0) + \delta \tilde{m}_{\pi, \text{mes}}^2, \tag{A.19}$$

where the counterterm is calculated from Eq. (2.9c). As a result we obtain

$$\Sigma_{\pi, \text{mes}}(0) = 3i\lambda^2 \int \frac{d^4k}{(2\pi)^4} \left(\Delta_{\sigma} - \Delta_{\sigma f} - (\Pi_{\sigma F} - \Pi_{\sigma F}^{(-1)} + \delta_{\sigma}) \Delta_{\sigma f}^{2} \right), \tag{A.20}$$

where $\Pi_{\sigma F}^{(-1)}$ is defined by Eq. (2.48a). Expressing Δ_{σ} as in (A.17b), the numerical evaluation of (A.20) presents no difficulties. As explained in the main text, $\Delta_{\sigma f}$ is approximated by its lowest order form, and meson–nucleon vertex form factors are multiplied to the self-energies. The corresponding self-energy of the σ meson is then calculated by numerical differentiation according to the formula (compare Eq. (A.16))

$$\Sigma_{\sigma, \text{mes}}(0) = \frac{\partial}{\partial \tilde{v}} (\tilde{v} \Sigma_{\pi, \text{mes}}(0)). \tag{A.21}$$

If all polarizations in are neglected, (A.20) and (A.21) reduce to the Hartree expressions given in Eqs. (3.8).

APPENDIX B

 $k \rightarrow 0$ Limits of the Polarizabilities

In the limit of small k, the forms of the density parts of the polarizations in Eqs. (2.32) and (2.35) are $\lceil 14 \rceil$

$$\frac{\Pi_{\sigma D}}{m_{\sigma}^{2}} = \frac{\delta_{\sigma}}{m_{\sigma}^{2}} + F_{\sigma}(C_{\sigma} - \phi(s))$$
(B.1)

$$\frac{\Pi_{\rm LD}}{m_{\omega}^2} = -F_{\omega}(1 - s^2 v_{\rm F}^2) \,\phi(s) \tag{B.2}$$

$$\frac{\Pi_{\rm M}^2}{m_{\sigma}^2 m_{\omega}^2} = F_{\sigma} F_{\omega} (1 - s^2 v_{\rm F}^2) \, \phi^2(s) \tag{B.3}$$

$$\frac{\Pi_{\rm TD}}{m_{\rm ev}^2} = F_{\omega} \frac{v_{\rm F}^2}{2} (1 - (1 - s^2) \,\phi(s)). \tag{B.4}$$

Here we used the notations

$$F_{\sigma} = N_{\rm F}^{(H)} (1 - v_{\rm F}^2) \frac{g^2}{m_{\sigma}^2}, \qquad F_{\omega} = N_{\rm F}^{(H)} \frac{g_{\omega}^2}{m_{\omega}^2}$$
 (B.5)

with

$$N_{\rm F}^{(H)} = \frac{2v_{\rm F}E_{\rm F}^2}{\pi^2}, \qquad v_{\rm F} = \frac{p_{\rm F}}{E_{\rm F}}, \qquad E_{\rm F} = \sqrt{p_{\rm F}^2 + \tilde{m}_{\rm N}^2};$$
 (B.6)

$$C_{\sigma} = 1 + \frac{1}{2} \frac{1}{1 - v_{\rm F}^2} - \frac{3}{4v_{\rm F}} \ln\left(\frac{1 + v_{\rm F}}{1 - v_{\rm F}}\right);$$
 (B.7)

$$\phi(s) = 1 - \frac{s}{2} \left(\ln \left| \frac{1+s}{1-s} \right| - i\pi\theta(1-|s|) \right), \qquad s = \frac{k_0}{|\mathbf{k}| v_F}.$$
 (B.8)

If $k_0 \to 0$ followed by $|\mathbf{k}| \to 0$, we have $s \to 0$ and $\phi \to 1$. If $|\mathbf{k}| \to 0$ followed by $k_0 \to 0$, then $s \to \infty$, $\phi \to 0$, and $s^2 \phi \to -\frac{1}{3}$. If we use (B.1) to (B.4) in (2.33a) we obtain

$$\varepsilon_{\rm L} = \frac{m_{\sigma}^{*2} + \Sigma_{\sigma \rm F}(0)}{m_{\sigma}^{2}} \left[1 - \frac{F_{\sigma} \phi}{(m_{\sigma}^{*2} + \Sigma_{\sigma \rm F}(0))/m_{\sigma}^{2}} + F_{\omega} \phi (1 - s^{2} v_{\rm F}^{2}) \right]$$
(B.9)

with the quasiclassical σ meson mass parameter

$$m_{\sigma}^{*2} = m_{\sigma}^{2} + \lim_{k_{0} \to 0} \lim_{|\mathbf{k}| \to 0} \Pi_{\sigma D}(\mathbf{k}) = \tilde{m}_{\sigma}^{2} + m_{\sigma}^{2} F_{\sigma} C_{\sigma},$$
 (B.10)

which agrees with Eq. (2.61a). By first setting $|\mathbf{k}| = 0$ or $k_0 = 0$ in (B.9) we obtain the two limits (2.60a), (2.60b). The transverse polarizability becomes in the $k \to 0$ limit

$$\varepsilon_{\rm T} = 1 + F_{\omega} \frac{v_{\rm F}^2}{2} (1 - (1 - s^2) \phi(s)).$$
 (B.11)

APPENDIX C

Wick Rotated Forms of the Density Parts of the Meson Self-energies

The density parts of the meson self-energies have been given analytically in Ref. [14]. The Wick rotated forms $(k_0 \rightarrow i\omega)$ are as follows, using $l^2 = \omega^2 + k^2$ with k the magnitude of the 3-momentum,

$$\Pi_{\sigma D} = \frac{g^2}{(2\pi)^3} \left(\rho_{\sigma} - (4\tilde{m}_N^2 + l^2) I_0 \right) \tag{C.1}$$

$$\Pi_{\rm LD} = \frac{l^2}{k^2} \frac{g_{\omega}^2}{(2\pi)^3} \left(-\rho_{\sigma} + k^2 I_0 - I_2 \right) \tag{C.2}$$

$$\Pi_{\rm M}^{2} = \frac{l^{2}}{k^{2}} \left(\frac{gg_{\omega}}{(2\pi)^{3}} 2\tilde{m}_{\rm N} I_{1} \right)^{2} \tag{C.3}$$

$$\Pi_{\rm TD} = \frac{g_{\omega}^2}{(2\pi)^3} \left(\frac{k^2 - \omega^2}{2k^2} \rho_{\sigma} + \frac{1}{2} \left(-\frac{l^2}{k^2} I_2 + (4\tilde{m}_{\rm N}^2 - l^2) I_0 \right) \right)$$
 (C.4)

with

$$\rho_{\sigma} = \int_{0}^{p_{\rm F}} d^3q \, \frac{4}{\tilde{E}_q} = 8\pi \left(p_{\rm F} E_{\rm F} - \frac{\tilde{m}_{\rm N}^2}{2} \ln \left(\frac{E_{\rm F} + p_{\rm F}}{E_{\rm F} - p_{\rm F}} \right) \right), \tag{C.5}$$

$$\tilde{E}_{q} = \sqrt{\tilde{m}_{N}^{2} + q^{2}}, \qquad E_{F} = \sqrt{\tilde{m}_{N}^{2} + p_{F}^{2}},$$
 (C.6)

$$I_0 = \frac{\pi}{k} \left[2E_F L_1 + \omega L_2 + 2k \ln \left(\frac{E_F + p_F}{E_F - p_F} \right) - \alpha L_3 \right]$$
 (C.7)

$$I_{1} = \frac{\pi}{2k} \left[(4E_{F}^{2} - \omega^{2} - \alpha^{2})L_{1} + 4E_{F}\omega L_{2} + 8kp_{F} \right]$$
 (C.8)

$$I_2 = \frac{\pi}{3k} \left[(8E_F^3 - 6E_F\omega^2) L_1 + (12E_F^2\omega - \omega^3) L_2 \right]$$

+2(
$$k^3 + 6\tilde{m}_N^2 k$$
) ln $\left(\frac{E_F + p_F}{E_F - p_F}\right) - \alpha^3 L_3 + 8p_F E_F k$. (C.9)

Here α and the L_i are given by

$$\alpha = k \sqrt{1 + 4\tilde{m}_{N}^{2}/l^{2}}$$
 (C.10)

$$L_1 = \ln \left[\frac{(E_+^{(-)2} + \omega^2)(E_+^{(+)2} + \omega^2)}{(E_-^{(-)2} + \omega^2)(E_-^{(+)2} + \omega^2)} \right]$$
 (C.11)

$$L_{2} = 2 \left[\operatorname{arctg} \left(\frac{E_{+}^{(+)}}{\omega} \right) - \operatorname{arctg} \left(\frac{E_{+}^{(-)}}{\omega} \right) + \operatorname{arctg} \left(\frac{E_{-}^{(-)}}{\omega} \right) - \operatorname{arctg} \left(\frac{E_{-}^{(+)}}{\omega} \right) \right]$$
(C.12)

$$L_{3} = \ln \left| \frac{(E_{+}^{(+)} - \alpha)(E_{-}^{(-)} - \alpha)(E_{-}^{(+)} + \alpha)(E_{+}^{(-)} + \alpha)}{(E_{-}^{(+)} - \alpha)(E_{+}^{(-)} - \alpha)(E_{+}^{(-)} + \alpha)(E_{-}^{(-)} + \alpha)} \right|, \tag{C.13}$$

and the $E_{\pm}^{(\pm)}$ are defined as

$$E_{\pm}^{(+)} = E_{p_{\rm F} \pm k} + E_{\rm F}$$
 (C.14)

$$E_{+}^{(-)} = E_{p_r+k} - E_F.$$
 (C.15)

One may verify explicitly that for any $l = (\omega, k)$ there are no singularities in the polarizations (C.1) to (C.4).

The above forms of the Wick rotated polarizations have been checked by numerical calculation as follows: According to Eq. (2.45a)

$$E_{(1)}^{\text{ex}} + E_{(2)}^{\text{ex}} = \delta E_{2D} + i \frac{\tilde{m}_{\text{N}}}{m_{\text{N}}} \bar{\Sigma}_{\text{Nf}} \Big|_{E = m_{\text{N}}} \int \frac{d^4k}{(2\pi)^4} \operatorname{Tr} S_{0D},$$
 (C.16)

where $\delta E_{\rm 2D}$ is given by Eq. (2.42d). In the calculation described in the main text, the exchange energies $E_{(1)}^{\rm ex}$, $E_{(2)}^{\rm ex}$ were calculated from Eqs. (2.45b), (2.45c). Likewise,

we can calculate the RHS of (C.16) directly by performing a Wick rotation in the integral (2.42d) and using the Wick rotated forms of the polarizations given above. If we introduce a meson-nucleon vertex form factor as described in the main text, both terms on the RHS of (C.16) are individually finite. The numerical calculation of the RHS of (C.16) agreed with the LHS calculated from Eqs. (2.45b), (2.45c), which confirms the analytical expressions (C.1) to (C.4).

REFERENCES

- 1. T. D. LEE AND M. MARGULIES, Phys. Rev. D 11 (1974), 1591.
- S. A. CHIN, Ann. Phys. (N.Y.) 108 (1977), 301; B. D. SEROT AND J. D. WALECKA, "Advances in Nuclear Physics," Vol. 16 (J. W. Negele and E. Vogt, Ed.), P. 1, Plenum, New York, 1985.
- A. D. Jackson, M. Rho, and E. Krotscheck, Nucl. Phys. A 407 (1983), 495; M. Prakash and T. L. Ainsworth, Phys. Rev. C 36 (1987), 346.
- 4. W. BENTZ, L. G. LIU, AND A. ARIMA, Ann. Phys. (N.Y.) 188 (1988), 61.
- 5. B. W. LEE, "Chiral Dynamics," Gordon & Breach, New York, 1972; J. MIGNACO AND E. REMIDDI, Nuovo Cimento A 1 (1971), 376.
- A. K. KERMAN AND L. D. MILLER, in "Second High Energy Heavy Ion Summer Study," LBL-3675, 1974.
- M. WAKAMATSU AND A. HAYASHI, Prog. Theor. Phys. 63 (1980), 1688; T. MATSUI AND B. D. SEROT, Ann. Phys. (N.Y.) 144 (1982), 107.
- 8. E. NYMAN AND M. RHO, Nucl. Phys. A 268 (1976), 408.
- L. G. Liu, "Quantum Effects in the Chiral σ-ω Model of Nuclear Matter," PhD. thesis, University of Tokyo, 1989.
- M. K. BANERJEE AND T. D. COHEN, "The Relativistic Random Phase Approximation and Mean-Field Descriptions of Nuclear Matter," University of Maryland Preprint 88-174, 1988.
- 11. S. ICHII, W. BENTZ, A. ARIMA, AND T. SUZUKI, Nucl. Phys. A 487 (1988), 493.
- 12. T. MATSUI, Nucl. Phys. A 370 (1981), 365.
- P. J. REDMONT, *Phys. Rev.* 112 (1958), 1404; N. N. BOGOLYUBOV, A. A. LOGUNOV, AND D. V. SHIRKOV, *Sov. Phys. JETP (Engl. Transl.)* 37 (1960), 574.
- 14. H. Kurasawa and T. Suzuki, Nucl. Phys. A 445 (1985), 685; 454 (1986), 527.
- 15. See, for example, S. O. BÄCKMAN AND W. WEISE, in "Mesons in Nuclei," Vol. III (M. Rho and D. Wilkinson, Eds.), p. 1095, North-Holland, Amsterdam, 1979.